Comparison of forest fire severity classification models based on aerial images and Landsat 8 OLI/TIRS images of a forest fire area in central Sweden

Foto: Amanda Löfdahl

Adrian Straker

Work Report 452 2016
Master thesis 30hp A2E

Handledare:
Jonas Bohlin

Sveriges lantbruksuniversitet
Institutionen för skoglig resurshushållning
901 83 UMEÅ
www.slu.se/srh
Tfn: 090-786 81 00

ISSN 1401–1204
ISRN SLU–SRG–AR–452–SE

Comparison of forest fire severity classification models based on aerial images and Landsat 8 OLI/TIRS images of a forest fire area in central Sweden

Adrian Straker

Keywords: Forest fire, Fire severity, Stereo Photogrammetry, Digital Surface Model, Aerial Images, NDVI, NBR, Image Matching, Västmanland

Master thesis in Forest Management at the dept. of Forest Resource Management
EX0768, A2E
Supervisor: Jonas Bohlin, SLU, Dept. of Forest Resource Management, Remote sensing
Examiner: Håkan Olsson, SLU, Dept. of Forest Resource Management, Remote sensing

---

Sveriges lantbruksuniversitet
Institutionen för skoglig resurshushållning
Utgivningsort: Umeå
Utgivningsår: 2016

ISSN 1401–1204
ISRN SLU–SRG–AR–452–SE

Acknowledgement

This thesis would not be present without the support of many people. Thus I would like to thank Jonas Jonzén for the support regarding data processing, Peder Axensten for normalizing the created point clouds, Anders Muszta for his statistical advises, Anton Grafström for his support considering the stratification of the data and Heather Reese for providing me information about random forest, all at the Swedish University of Agricultural Sciences in Umeå Sweden. Furthermore I would like to thank all my fellow students I worked with in the laboratory for the support and the great and friendly atmosphere, even in stressful times. And especially I would like to thank my supervisor Jonas Bohlin for providing me the opportunity to work on the project and his support in both organisational and subject-specific questions.

Summary

Due to different level of fire severity a diverse mosaic of vegetation pattern establishes after the occurrence of a forest fire. In order to study the effects of forest fires and to plan future remediation of the burned area remote assessment of forest fire severity has shown to be a valuable tool. This classification is usually performed by using spectral indices derived from satellite images. However constrains and inconsistent results are reported for the commonly used approaches. Thus a test on other data sources in order to classify forest fire severity is stressed by other studies. Particularly the integration of spatial characteristics, such as height metrics of burned forest areas into classification models seems to be promising. Thus the aim of the present study is to create new fire severity classification model approaches integrating both spatial metrics derived from pre and post fire aerial images using stereo photogrammetric techniques and spectral metrics of these aerial images of a forest fire in Västmanland (central Sweden). Accordingly six different model approaches integrating different compositions of spatial and spectral metrics derived from pre and post fire aerial images were created using random forest as a classification algorithm. Furthermore 3 classification models based on a post fire Landsat 8 OLI/TIRS scene using ordinal regression and already applied classification approaches were created as comparison. The performances of all created models were assessed by the application of all models on test data sets, the generation of confusion matrices and finally the computation of the overall accuracy and the Cohen´s Kappa values. It can be summarized that both models integrating spatial metrics derived from aerial images show the lowest overall accuracies (47,15 % and 50,10 %) and Cohen´s Kappa values (0,26 and 0,31). Furthermore the models integrating metrics or indices derived or computed from the post fire Landsat 8 scene show substantial overall accuracies and Cohen´s Kappa values. Additionally the models integrating spectral metrics derived from aerial images show moderate to substantial overall accuracies and Cohen´s kappa values, whereas the highest overall accuracy (82,32 %) and Cohen´s Kappa value (0,75) is achieved by the model integrating only spectral metrics derived from post fire aerial images. Thus it is to conclude that spatial metrics derived from aerial images using stereo photogrammetric techniques seem to be not suitable for the classification of forest fire severity. However spectral metrics derived from post fire aerial images seem to be promising in order to classify forest fire severity and might lead to good results in combination with ALS data derived spatial metrics of burned forest areas. Furthermore this study shows strong correlations between forest fire severity and the thermal bands of Landsat 8 TIRS, which might be studied in future research.

Table of Content

1 Introduction 1
1.1 Issue and purpose 3
2 Material and methods 6
2.1 Study area 6
2.2 Data sources 7
2.2.1 Aerial images 7
2.2.2 Landsat 8 OLI/TIRS scene 8
2.2.3 Setup of infield data collection and assessment of sample plots 9
2.2 Pre-processing data 9
2.2.1 Pre-processing aerial images 9
2.2.2 Pre-processing Landsat 8 scene 11
2.2.3 Stratification and splitting generated data sets in training and test data sets 12
2.3 Model creation 12
2.3.1 Model creation based on data set (a) including metrics derived from post fire aerial images 13
2.3.1.1 Random forest 13
2.3.2 Model creation based on data set (c) including the difference of spectral and spatial metrics derived from both pre and post fire aerial images 15
2.3.3 Model creation based on data set (d) including metrics derived from post fire Landsat 8 scene 16
2.4 Error analysis and prediction on test data sets 16
2.4.1 Cohen´s Kappa 17
3 Results 18
3.1 Correlation of variables 18
3.2 Model creation 21
3.2.1 Model based on metrics derived from post fire aerial images 21
3.2.2 Model based on difference metrics computed from pre and post fire aerial images 22
3.2.3 Model based on metrics derived from post fire Landsat 8 scene 24
3.3 Classification accuracy 24
3.3.1 Internal accuracy assessment of the random forest models 24
3.3.2 Application of models on test data sets 25
4 Discussion 28

5 Outlook future research 32
References 33
Appendix 38

Table of tables

Table 1. Landsat 8 Operational Land Imager (OLI) and Thermal Infrared Sensor (TIRS) 8
Table 2. Tested model settings (number of trees and variables used at each split) of the random forest models integrating either metrics derived from post fire aerial images or difference metrics computed from post and pre fire aerial images 15
Table 3. The highest calculated spearman´s correlation coefficients (Rho) between fire severity and spectral variables derived from post fire aerial images and all calculated spearman´s correlation coefficients (Rho) between fire severity and spatial variables derived from post fire aerial images 19
Table 4. The highest calculated Spearman´s correlation coefficients (Rho) between fire severity and difference spectral variables computed from pre and post fire aerial images and all calculated Spearman´s correlation coefficients (Rho) between fire severity and difference spatial variables computed from pre and post fire aerial images 20
Table 5. Spearman´s coefficient (Rho) between fire severity and spectral and thermal metrics and spectral indices derived or computed from the post fire Landsat 8scene 21
Table 6. Settings of the random forest algorithm for Ntree, sample size and mtry of the classification models including metrics derived from post fire aerial images ..22
Table 7. Variable importance (mean decrease gini) of the 10 most important metrics of each model based on metrics derived from post fire aerial images 22
Table 8. Settings of the random forest algorithm for Ntree, sample size and mtry of the classification models including difference metrics computed from pre and post fire aerial images 23
Table 9. Variable importance (mean decrease gini) of the 10 most important metrics of each model based on difference metrics computed from pre and post fire aerial images 23
Table 10. Out of bag (OOB) overall accuracy of the computed random forest models integrating metrics derived from post fire aerial images and integrating difference metrics computed from pre and post fire aerial images 24
Table 11. User´s, producer´s and overall accuracy by class of the computed classification models integrating metrics derived from aerial images and the Landsat 8 scene applied on test data sets 26
Table 12. Cohen´s Kappa values of the computed classification models based on metrics derived from aerial images and the Landsat 8 scene applied on test data set 27
Table 13. Confusion matrix of the best performing classification model integrating spectral metrics derived from post fire aerial images applied on test data set 27

Table of figures

Figure 1. Location of the forest fire area in Västmanland central Sweden on the left, and a Landsat 8 OLI/TIRS scene of the forest fire area on the right (acquired 14th Sep. 2014).....7

1 Introduction

Forest fires are considered to be the most important source of natural disturbances in the boreal forest (Wein 1993) and its effects on ecosystem processes in the boreal forest are well studied. After the occurrence of fire, a mosaic of vegetation patterns is created due to different levels of fire severity whereas also surface relief, exposition, vegetation type and edaphic conditions have a post fire effect on vegetation pattern (Zackrisson 1977). Accordingly forest fires contribute to diversity on different spatial scales in the boreal forest (Suffling et al. 1988; Angelstam 1998; Bergeron et al. 2002) and the severity of a forest fire has an effect on forest productivity even centuries after fire occurrence (Burton et al. 2008). Rees & Juday (2002) report an increased floristic richness in burned forests than in logged forests of similar development stage in the boreal forest in Alaska. Furthermore differences in mycorrhizal fungi (Dahlberg et al. 2001), insects (Wikars & Schimmel 2001) and vascular vegetation (Schimmel & Granström 1996, Chapin et al. 2006) are reported as a result of the occurrence of different fire severities. The occurrence of various fire severity levels is attributed to different pre fire forest and site characteristics (Burton et al. 2008).

In the year 1933 particularly many forest fires occurred in Sweden within the last century (Zackrisson 1977). Nevertheless there was a major decrease both in burned area-size and fire frequency in the end of the 19th century, due to snag removal and successful fire control (Zackrisson 1977). The largest documented fire occurred 1694 with a size of approximately 7000 ha in the eastern part of the county Västerbotten contiguous to the Ume river (Tirén 1937; Esseen et al. 1997). Furthermore there is a north-south gradient in fire occurrence recognizable in Sweden, whereas higher fire frequencies occur in the south (Granström 1993). Recent studies state that the climate change will have a promoting effect on the occurrence of forest fires in the boreal forest in the future and thus significant ecosystem changes induced by an altered fire regime are likely to occur (Stocks et al. 1998; Wotton et al. 2010). Therefore particularly forest managers, ecologists and scientists are in need of a useful tool to gain knowledge about forest fires effects and to plan post fire forest remediation and further measures now and in the future.

In order to describe the variation of forest fire effects within a burned area and to map forest fire regimes the assessment of fire severity is widely used (Chafer et al. 2004; Roy et al. 2006; Morgan et al. 2001). Although several definitions of fire severity are discussed and the term itself is used heterogeneously in several contexts, it basically relates to the loss of biomass above- and belowground after fire occurrence (Keeley 2009). Due to identifiable post fire spectral changes and difficulties in the execution of traditional methods remote sensing has shown to be a valuable tool to asses and map fire severity (Chafer et al. 2004; Hammill & Bradstock 2006; Escuin et al. 2008). Consequently, particularly spectral metrics and calculated indices based on these metrics derived from Landsat TM/ETM images are used (Escuin et al. 2008; Miller & Yool 2002; French et al. 2008).

One frequently applied and tested index also in the boreal forest is the Normalized Differenced Vegetation Index (NDVI), which relies on the combination of red and near infrared (NIR) regions to differentiate burned from unburned areas (Chafer et al. 2004; Epting et al. 2005; Escuin et al. 2008; Keeley et al. 2008; Miller & Yool 2002). Several studies show that the NDVI is sensitive to spectral changes caused by fire (Hammill & Bradstock 2006; Escuin et al. 2008).

Contrary to the NDVI approach various other studies integrate post fire changes of the mid or short wave infrared (MIR / SWIR) region in combination with the NIR region into the assessment of fire severity by computing the Normalized Burn Ratio (NBR).
Using Landsat TM/ETM+ images Epting et al. (2005) evaluate different remotely sensed indices on four burned sites in Alaska. Their results indicate a high consistent performance of NBR-correlation with in-field assessments of fire severity, namely Composite Burn Index (CBI). Whereas the NBR was particularly highly correlated to burn severity in classifications using only forest displaying pixels and forested classes.

Also Escuin et al. (2008) report by analysing Landsat TM/ETM images of three burned sites in Spain that the NBR is highly sensitive to post fire spectral changes. However, these results are not supported by Roy et al. (2006), who processed Landsat TM/ETM+ images from the South African savanna and MODIS images from the Australian savanna, Russian Federation boreal forest and South American tropical forest to map fire severity levels by using the NBR. They found no evidence of optimal NBR performance in analysing fire severity after fire occurrence. Considering those findings Escuin et al. (2008) discuss that including unburned and burned pixels in the calculation conducted by Roy et al. (2006) is a probable reason for the poor optimality of the NBR. By comparing the results of NDVI- and NBR- fire severity assessment studies indicate a higher correlation of NBR and in field-assessment of fire severity than the latter and NDVI (Epting et al. 2005, Escuin et al. 2008, Hoy et al. 2008). Above presented studies analysed and applied the indices basically in a uni-temporal (post-fire) manner. However, both NDVI and NBR are also used in a bi-temporal approach (post-fire/pre fire differences), which is indicated by a minuscule “d” (dNDVI, dNBR) (Escuin et al. 2008, French et al. 2008).

By analysing Landsat TM/ETM images in southern Spain Escuin et al. (2008) report considering the applicability of the dNDVI that named index shall be rather used to discriminate burned from unburned pixels than to discriminate between different fire severity levels, due to better results of the application of dNBR and NBR. In a comparative study French et al. (2008) review fire severity assessments in the boreal forest in North America based on in-filed fire severity assessments using CBI and dNBR. They conclude that various studies demonstrate an overall high level of correlation between dNBR and CBI. In contrast to their conclusion Hoy et al. (2008) and French et al. (2008) present restrains of the dNBR approach in the Alaskan boreal region.

Besides NDVI and NBR and their bi-temporal counterparts further indices exist, which basically combine similar to the NDVI Red and NIR regions to assess and map fire severity. For instance Chuvieco et al. (2002) tested the Burnt Area Index (BAI) using Landsat TM and NOAA Advanced Very High Resolution Radiometer (AVHRR) images of burned areas in Mediterranean countries (Italy, Greece, Spain) and compared the results to other vegetation indices such as NDVI, Soil Adjusted Vegetation Index (SAVI) and Global Environmental Monitoring Index (GEMI). The equations of the named indices BAI, SAVI and GEMI are presented in the appendix.

Chuvieco et al. (2002) conclude that the BAI has a greater sensitivity to burned areas than the other tested indices. However, there are probable disarrays with low-reflectance areas such as water bodies, since the BAI was developed to emphasise charcoal areas. Furthermore the BAI was designed for Mediterranean environments and its applicability is mainly dependent on post-fire endurance of charcoal (Chuvieco et al. 2002). A different approach, which is not limited to two spectral regions, was applied by Michalek et al. (2000). They used Landsat TM images to estimate carbon release from a fire in an Alaskan spruce forest. For this purpose they integrated band 1 – 5 and 7 in their classification process and created an accurate severity map. However they further state that band 4 and 5 (NIR and Red) have been proven to be the most important regions. This fact would support the use of indices relying on red and NIR regions as described above. Nevertheless also Rogan & Franklin (2001) show that a multispectral classification method leads to valuable results and French et al. (2008) conclude that the use of several spectral regions may be better than the limited use of only two bands combined within an index.

1.1 Issue and purpose

Although presented indices and approaches are all applied to assess fire severity and positively tested, also inconsistencies, constrains and poor results are reported. Thus it is discussed whether spectral indices are suitable to operate sufficiently on different sites within and among biomes (Roy et al. 2006; Hoy et al. 2008; Allen & Sorbel 2008; French et al. 2008). Particularly reflectance variability of burned sites due to sun elevation angle and plant phenology are considered to be the main reasons why spectral indices are substantially influenced (Rogan & Franklin 2001; Verbyla et al. 2008) and why it may not be possible to design a spectral index which coincides the index theory (Roy et al. 2006). Regarding these considerations several studies suggest to refine already used methods or to look for new approaches within remote sensing to assess fire severity considering other post fire ecosystem responses than only altered spectral properties (Conard et al. 2002; Hammill & Bradstock 2006; Hoy et al. 2008; Keeley et al. 2008; Roy et al. 2006).

Taking these considerations into account, seeking for a new approach more insensitive to constrains of already existing methods, the present study tests different fire severity classification model approaches considering mainly the applicability of models based on spatial or spectral metrics or a combination of both derived from pre and post fire aerial images of a forest fire in Västmanland, central Sweden, whereas the main focus lies on classification models integrating spatial metrics derived from aerial images.

Thereby it needs to be considered that when spoken of spatial metrics it is actually referred to height metrics computed from 3D point clouds derived from aerial images of the burned area. In theory spatial forest characteristics such as forest height should be altered after occurrence of fire and thus relatable to different fire severity classes. Based on these assumptions it should be further possible to design fire severity classification models. The use of spatial metrics in order to classify and map forest fire severity is encouraged by Michalek et al. (2000), Rogan & Franklin (2001), Lentile et al. (2006) and French et al. (2008). Spatial metrics derived from Airborne Laser Scanning (ALS) data are already tested in order to classify fire severity (Montealegre et al. 2014). In their study Montealegre et al. (2014) testify a good applicability of spatial metrics.

However, in the present study it was decided to use a photogrammetric approach by using aerial images in order to classify fire severity. The reason that a photogrammetric approach is used and tested in the present study is mainly based on the objective to create an alternative to ALS data derived fire severity classification. This is mainly due to the fact that high acquisition costs of ALS data are considered as a primary disadvantage of using this data source for describing forest characteristics on a large scale (Næsset 2002).

Consequently the replacement of ALS data based approaches with stereo photogrammetric techniques in order to estimate forest characteristics is considered to deliver a cost effective alternative (Gobakken et al. 2015). Additionally recent studies have shown potentials of stereo photogrammetric techniques considering the analysis of forest variables (Næsset 2002; Heurich et al. 2003, Haala et al. 2010; Bohlin et al. 2012; Järnstedt et al. 2012; Gobakken et al. 2015) and Baltsavias et al. (2008) state that stereo photogrammetry is a valid alternative to methods based on ALS data. Furthermore Baltsavias (1999) states that ALS and photogrammetry shall be considered complementarily rather than competitive to create and maintain a versatile tool box to choose from in future applications.

In order to extract spatial metrics of aerial images Digital Surface Models (DSM) were created by using Semi Global Matching (SGM) in the present study. Regarding the use of DSM derived from aerial images Haala (2009) proclaims a comeback of this approach within the last years. Regarding the creation of DSM Semi Global Matching of aerial images is considered to be a suitable alternative to ALS data based DSM creation due to better cost efficiency (Gehrke et al. 2008). Rothermel & Haala (2011) prove that SGM is a resilient matching algorithm.

In the present study the results of classification models integrating spatial and spectral metrics derived from post fire aerial images are compared with the results of commonly used classification models based on NDVI, NBR and multispectral and thermal metrics derived from a post fire Landsat 8 Operational Land Imager (OLI) and Thermal Infrared Sensor (TIRS) scene. Furthermore pre fire aerial images are used in this study in order to analyse whether the integration of spatial and spectral metrics derived from aerial images from different time origins in classification models lead to an improved classification. The nine classification model-approaches built and tested in the present paper are summarized in the appendix in table 1.

Whereas classification approach 1, 2 and 3 include metrics derived from post fire aerial images and approach 4, 5 and 6 include both metrics derived from post and pre fire aerial images. The last three approaches integrate spectral and thermal metrics and spectral indices derived and computed from the Landsat 8 scene.

In summary the aims of this study are to 1) create and test the nine presented classification approaches considering the classification of fire severity of the forest fire area in Västmanland, 2) focus on testing the applicability of classification models based on spatial metrics derived from aerial images, 3) define the most suitable approach to classify fire severity of the nine tested approaches.

2 Material and methods

2.1 Study area

The study area is located in central Sweden in the county of Västmanland (Figure 1). Before fire occurrence mainly scots pine (*Pinus sylvestris*) and norway spruce (*Picea abies*) forests were occupying the area. Furthermore broadleaf dominated forests, with main tree species birch (*Betula sp.*) and European aspen (*Populus tremular*), and mixed deciduous-coniferous forests existed.

The forest fire occurred on an area of approximately 13.100 ha, of which approximately 9576 ha are considered as productive forest (wood production > $1m^3$ / ha, year) and 1485 ha as unproductive forest areas according to FAO definition. Residual areas are composed of mires (~ 1359 ha) according to FAO definition, rocky outcrop (~ 153 ha) according to FAO definition, water (~ 270 ha), farmland (~ 36 ha), roads (~ 162 ha), development areas (~ 27 ha) and forest roads (~ 9 ha). 98 % of the area is damaged by the fire. On 4 % of the area no damaged tree crowns are ascertained, on 23 % of the area tree crowns were damaged 50% or less, on 52 % of the area tree crowns were damaged 51% or more and on 25 % of the area crown fires occurred (no leaves / needles remaining). For more information about the burned area see Nilsson et al. (2014).

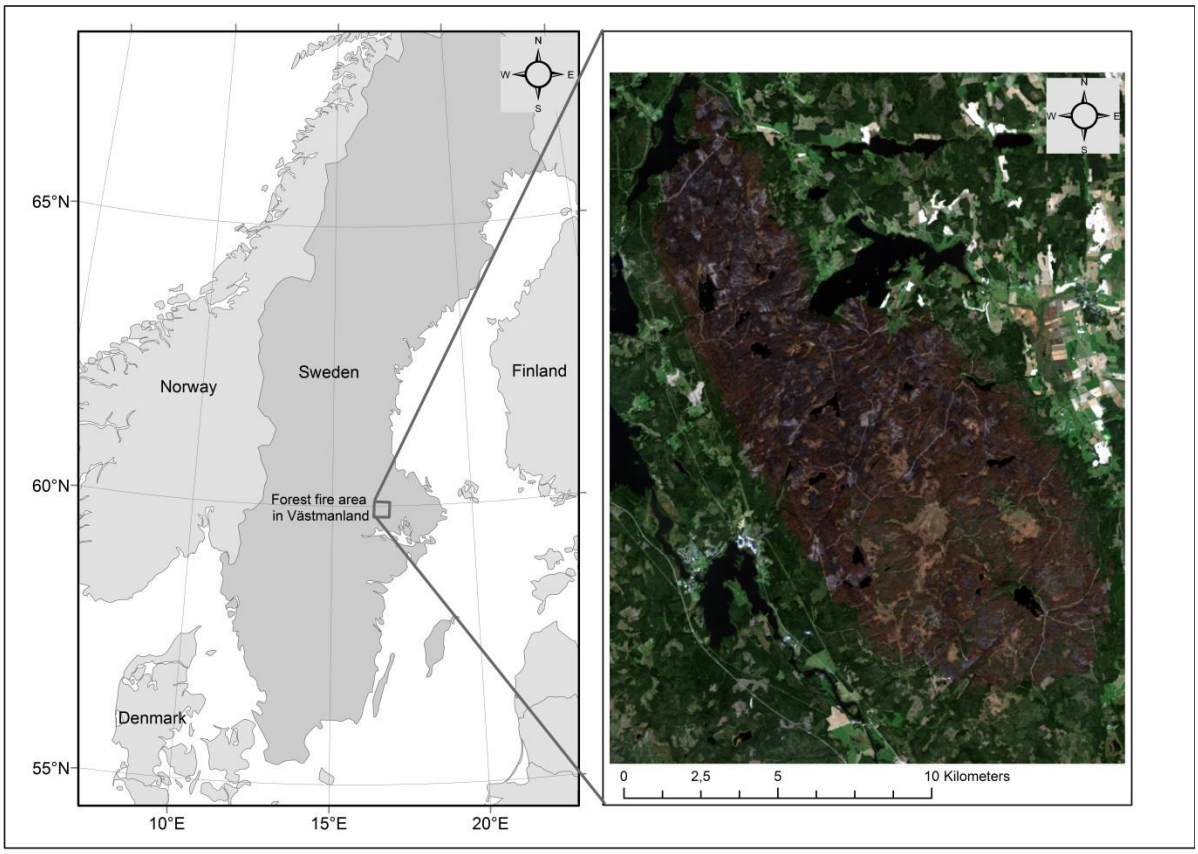

Figure 1. Location of the forest fire area in Västmanland central Sweden on the left, and a Landsat 8 OLI/TIRS scene of the forest fire area on the right (acquired 14th Sep. 2014).

2.2 Data sources

2.2.1 Aerial images

The aerial images used in this study have a ground sample distance of approximately 25 cm and were taken with a digital camera (Vexcel UltraCam Eagle) from an aircraft flying on the north-south axis on an elevation of 3700 metres above ground. Pre-processing of the aerial images was conducted by the Swedish Land Survey (Lantmäteriet). This Pre-processing involved a computation of the aerial images into a level-2 data format, which is a data format containing the digital negative of the camera. Furthermore exterior orientations for whole image blocks were generated and radiometric correction was conducted using a model based approach, which included correction of haze, atmospheric effects, hotspots and an adjustment of the final colour tone (Wiechert & Gruber 2011; Reitinger et al. 2012). Resulting in pan-sharpened Colour Infrared (CIR) images (Green, Red, Infrared) with an 8 bit radiometric resolution.

In total 106 post fire aerial images acquired on the 14th of August 2014 short after the occurrence of fire are included in the present study. Furthermore 111 pre fire aerial images acquired on different dates in spring / early summer 2014 are used for computations. The aerial images are taken with forward overlap of 60 % and sideward overlap of 30 %.

2.2.2 Landsat 8 OLI/TIRS scene

In the present study one sixteen bit Landsat 8 scene matching the forest fire area in Västmanland was used, whereas the used scene includes eleven bands of the OLI and TIRS of Landsat 8. However, only the multispectral OLI bands 2 to 7 and the thermal bands 10 and 11 of TIRS were included in further computations. Band 1, band 8 and band 9 were excluded because of their specific area of application (band 1: Coastal/aerosol analysation, band 8: Panchromatic, band 9: Cirrus detection). The distinct wavelengths of Landsat 8 OLI / TIRS bands are summarized in table 1. The scene was acquired on the 14th Sep. 2014 one month after fire occurrence and already pre-processed before it was purchased for the present study. Regarding this the scene was orthorectified, based on the Universal Transverse Mercator (UTM) map projection and georeferenced in the World Geodetic System (WGS) 84. Additionally the Ground sampling distance of all included Landsat 8 bands is 30 meters (m), whereas the bands 10 and 11 were collected at 100 m but resampled to 30 m. Further computations were not conducted.

Table 1. Landsat 8 Operational Land Imager (OLI) and Thermal Infrared Sensor (TIRS)

Band	Wavelength in micrometres (µm)	Ground sample distance in metres (m)
1 Coastal aerosol	0.43 - 0.45	30
2 Blue	0.45 - 0.51	30
3 Green	0.53 - 0.59	30
4 Red	0.64 - 0.67	30
5 Near Infrared (NIR)	0.85 - 0.88	30
6 Short Wave Infrared (SWR) 1	1.57 - 1.65	30
7 Short Wave Infrared (SWR) 2	2.11 - 2.29	30
8 Panchromatic	0.5 - 0.68	15
9 Cirrus	1.36 - 1.38	30
10 Thermal Infrared (TIRS) 1	10.60 - 11.19	100 (resampled to 30)
11 Thermal Infrared (TIRS) 2	11.50 - 12.51	100 (resampled to 30)

2.2.3 Setup of infield data collection and assessment of sample plots

The classification of fire severity required an assessment and collection of site characteristics. Particularly the in-field assessment of fire severity was needed in order to train and test the classification models. This data collection and the assessment of fire severity were conducted by Nilsson et al. (2014). In total 2062 sample plots with a radius of 10 m within a grid of 300 m times 300 m were positioned over the study area and remotely interpreted using the same aerial images used in the present study.

The interpretation of fire severity considers the degree of tree crown damage due to fire on four level from 0 to 3, whereas class 0 includes sample plots with only unburned tree crowns, class 1 is assessed for sample plots where tree crowns are damaged up to 49 % by fire, class 2 represents sample plots including tree crowns damaged by fire equal or greater than 50 % but less than total tree crown destruction and class 3 is assessed after occurrence of a crown fire without the survival of any leafs / needles.

Furthermore the land usage classes were assessed on sample plot level. Thereby nine land usage classes are discriminated. Besides named sample plot assessments 28 other site characteristics are analysed, which are not considered in the present study. Among these interpretations of site characteristics fire severity of the sample plots was also assessed on another scale. However due to the facts that this scale is assessing whether the ground is damaged by fire or not and the present study is focusing on the altered forest characteristics after fire occurrence it was decided to only include the assessment of fire severity based on tree crown damages.

2.2 Pre-processing data

2.2.1 Pre-processing aerial images

In order to base the assessment of fire severity on spatial and spectral metrics derived from aerial images of the burned forest in Västmanland, both pre and post fire aerial images were implemented with *INPHO* into one pre and one post fire project file. These project files included besides information about camera type, flight characteristics such as camera position and flight direction also information about the orientation of the aerial images, which are necessary information for the next step of applying SGM. SGM is an image matching algorithm based on pixel wise matching of Mutual Information and an important requirement for the creation of 3D reconstructions of images. The Mutual Information approach was developed in order to find the pose of an object in an image and to process complex radiometric relationships between images (Viola & Wells 1995). Basically while performing pixel wise matching semi global matching computes the matching costs of the relation of each base image pixel and each matching image pixel. Thereby a path wise optimization cost function is used aiming to minimize the global costs (Hirschmüller 2008). SGM was conducted by using *SURE version 1.2.1.210*. As a result several las files containing 3D point clouds of pre and post fire aerial images were created. Thereby default configurations in *SURE* were used except that *Aerial Nadir* (forward overlap: 60%; sideward overlap: 30 %) was used as *Scenario Type*. The 3D point clouds contained information about the spatial position and spectral characteristics (Values of Red, Green and NIR) of each point. Whereby, the spectral information of the 3D point clouds derived from the base images which were randomly defined and used by SURE for the matching process.

In order to extract spatial and spectral metrics from the generated 3D point clouds further computation was conducted. Accordingly all las files of each time origin were processed using *lasclip* of the software *lastools version 2.1*. During this step all 3D point clouds at the same location and with the same extension (radius 10 m) like the sample plots were extracted from the las files. Afterwards the clipped sample plot 3D point clouds of each time origin were merged into one post fire and one pre fire las file by using *lasmerge* of the software *lastools version 2.1*. As a direct pre step to the extraction of spatial and spectral metrics of both las files these files needed to be normalized. This normalization was conducted using the software pax-filter. The normalization was extracted using a Digital Elevation Model based on ALS data derived from the Swedish Land Survey. This DEM has a ground sample distance of 2 metres. However the slightly greater ground sampling distance of the ALS data derived DEM compared to the ground sampling distance of the used aerial images is considered to have no great impact on the classification results. In order to remove noise from the 3D point clouds of both the pre fire las file and the post fire las file all points above 50 metres and below -4 metres were removed and the points between 0 metres and -4 metres were summarized as new ground level on 0 metres during the normalization process.

Following by applying l*as2las* of the software *lastools version 2.1* on the newly created pre and post fire normalized 3D point cloud las files every 3D point cloud covering a sample plot was extracted into one distinct las file. Finally the spatial and spectral metrics of the generated pre and post fire 3D point cloud las files of every single sample plot were extracted with the package *CloudMetrics* included in *FUSION version 3.42*. Thereby all points above 2 metres were used to calculate the metrics. The spectral metrics were extracted from the generated 3D point clouds for each band (Green, Red, NIR) and stored in distinct tables for each band and time origin (pre and post fire). Also the spatial metrics were extracted from the generated 3 D point clouds and stored in distinct tables regarding the time origin (pre and post fire) after the extraction. Afterwards all redundant variables, either because they had no values or were of no need for further calculations were removed from all created tables.

By using the function *merge* of the package *Base version 3.1.0* in *R* all three pre fire spectral metric tables (Green, Red, NIR) and the pre fire spatial metric table were merged into one and all three post fire spectral metric tables (Green, Red, NIR) and the post fire spatial metric table into another table. Afterwards each of both resulting tables was combined with the forest characteristic and fire severity assessment described in section 2.2.3. Finally one data set of each time origin (pre and post fire) was produced including, for each sample plot, spatial and spectral metrics derived from either pre fire aerial images or post fire aerial images and the information about forest characteristics and fire severity. The data set including spectral and spatial metrics derived from post fire images in combination with the fire severity and forest characteristic assessment is referred to as data set (a) and the data set including spectral and spatial metrics derived from pre fire aerial images in combination with the fire severity and forest characteristic assessment is referred to as data set (b). Finally by subtracting the spatial and spectral variables derived from post fire aerial images (data set a) from the spatial and spectral metrics derived from pre fire aerial images (data set b) a differenced data set (c) was created.

2.2.2 Pre-processing Landsat 8 scene

For each of the eight Landsat 8 bands used in the present study one specific raster was created in *R* using the function *raster* of the package *Raster version 2.4-20*. Furthermore by processing the raster representing the NIR band and the Red band a new raster, in which each pixel represents one NDVI-value, was computed by applying following equation.

$$NDVI = \frac{(Band\ 5 - Band\ 4)}{(Band\ 5 + Band\ 4)}$$

The same step was applied using the SWR2 and the NIR band raster to compute a new raster including one specific NBR-value for each pixel with the following equation.

$$NBR = \frac{(Band\ 5 - Band\ 7)}{(Band\ 5 + Band\ 7)}$$

Afterwards the spectral metrics of each band raster, the NDVI raster and the NBR raster were extracted on plot level using the function *extract* of the *R* package *Raster version 2.4-20* and merged with the remotely sensed assessment of forest characteristics and fire severity into one data set by using the function *merge* of the package *Base version 3.1.0* in *R*. This data set is in the following referred as data set (d). Due to the fact that the ground sample distance of 30 m of the Landsat 8 scene exceeded the size of the sample plots, nearest neighbour was applied in order to extract the spectral values of each pixel. Thus the assessment of fire severity was extrapolated on pixel size of the Landsat 8 scene and thus the ground sampling distance of the future classification map was set.

2.2.3 Stratification and splitting generated data sets in training and test data sets

Due to the fact that following classifications are supposed to describe the fire severity of only forested areas, non-forest sample plots and their extracted spectral and spatial values were excluded from the data sets (a), (c) and (d). Thus only sample plots and their metrics of the land usage classes "productive forest" (Ägoslag1) and "unproductive forest" (Ägoslag9) were included in further computations.

Furthermore in order to train and to test the efficiency of the computed classification models each of the three data sets (a, c, d) was divided into two data sets, whereas the training data sets included 70 %, the test data sets 30 % of the sample plots. The division was executed by using the *local pivotal method 1* in the package *Balanced Sampling version 1.4* in *R* (Grafström 2016), aiming for balanced training respectively test data sets depending on the spatial distribution and the pre-assessed fire severity level of included sample plots. Accordingly the ratio of the fire severity levels was identical in the training respectively test data sets as in the undivided original data sets and sample plots within both training and test data sets were equally distributed over the fire area.

2.3 Model creation

In all models computed in the present study the dependent variable is categorical on an ordinal scale and all spatial, spectral and computed independent variables are continuous. Therefore it was necessary to decide on a model algorithm which can handle categorical data. However before model creation the data in the three data sets (a), (c) and (d) was analysed statistically, whereas the independent variables of each data set (data set a, c and d) were tested on normality (Shapiro Wilk test; $\alpha = 5\%$) using the function *shapiro.test* of the *R* package *Stats version 3.1.0* and the spearman correlation coefficients using the function *rcorr* included in the *R* package *Hmisc version 3.17-0* of all independent variables were calculated. Besides that each spectral and spatial metric derived from post fire aerial images included in data set (a) was compared to the equivalent metric derived from pre fire aerial images included in data set (b) by applying the Wilcoxon signed rank test ($\alpha = 5\%$) in order to assess which metrics are significantly altered after the occurrence of fire. This test was applied using the function *wilcox.test* of the *R* package *Stats version 3.1.0*. The decision to use the Wilcoxon signed rank test was based on the results of the test on normality of the independent metrics and because a paired relationship of pre and post fire aerial image derived metrics was expected.

Furthermore the independent variables of the data sets used for model creation (data set a, c and d) were assessed visually to determine specific variable patterns considering the fire severity classes.

2.3.1 Model creation based on data set (a) including metrics derived from post fire aerial images

The test on normality (Shapiro Wilk test; $\alpha = 5\%$) showed that all independent spectral and spatial variables derived from post fire aerial images included in data set (a) are not normally distributed. Furthermore the calculation of the spearman's correlation coefficient among all independent variables of the data sets (a) showed that several variables in this data set are correlated with each other. Therefore and due to the amount of different variables there is a possibility of multicollinearity of the data. Thus it was necessary to draw on a model which is resilient towards multicollinearity and not normally distributed variables. Those considerations resulted in the decision to use the random forest algorithm as classification model.

2.3.1.1 Random forest

Random forest in classification mode is an algorithm based on combinations of tree classifiers,

$$\{h(x, \theta_k), k = 1, \dots, \}$$

where x is an input pattern of variables and $\{\theta_k\}$ are independent identically distributed random vectors (Breiman 2001).

Every tree is thereby trained on a random sample (bootstrap sample), which is drawn with replacement of the training or original data set. This step is called bagging. In order to determine the most efficient node splits and node sizes of each tree a randomly sampled set of independent variables is used. Due to the fact that only a subset of independent variables is used at each split random forest shows reduced computational complexity. Thus it is considered to be lighter than conventional bagging of other tree type classifiers (Gislason et al. 2006). Furthermore the correlation among trees is reduced by sub setting the input variables. Also pruning of trees is obsolete, which is considered to be the major advantage compared to similar tree classifiers (Quinlan 1993). In random forest each generated tree casts one classification for one pattern of input variables. Consequently the prediction on new data is based on the majority vote of trees in the forest. Furthermore an internal model performance assessment is carried out by random forest. Whereby, the out of bag (OOB) data which was excluded from the classification after bagging is used to estimate the generalization error by performing internal cross validation (Gislason et al. 2006). Furthermore random forest offers an included assessment of variable importance. Whereas two of the most commonly used assessments of variable importance are either based on the Gini impurity criterion or conducted by the application of the Permutation importance (Breiman 2001). The latter compares the prediction accuracy of a tree after permutation of an input variable. These permutations are conducted for all trees of the forest. If the permutations result in an increased generalized error, the importance of the variable of interest is indicated (Gislason et al. 2006). The Gini impurity criterion measure describes mainly the impurity of a given element or attribute with respect to other classes (Pal 2005, Rodriguez-Galiano et al. 2012).

In order to describe variable importance based on the Gini impurity criterion similar to the permutation importance approach random forest permutes one input variable at a time and measures the decrease of accuracy by mean of the Gini impurity criterion (Rodriguez-Galiano et al. 2012).

Random forest is considered to be relatively robust towards outliers and noise (Breiman 2001). Finally random forest can use large numbers of trees and handle high dimensional input variables. Therefore and due to the fact that random forest can deal with correlations and complex interactions between variables it shows high popularity in classification applications (Hapfelmeier et al. 2014). Furthermore the random forest algorithm is suitable for multi-class problems, does not over fit and can handle both categorical and continuous data (Díaz-Uriarte & Alvarez de Andrés 2006). These facts were the main reason to use random forest in the present study, as indicated above.

Three different models based on metrics derived from post fire aerial images were computed. Thereby the first model includes all spatial and spectral metrics, the second model includes only spatial metrics and the third model includes only spectral metrics. For the computation of the models the function *RandomForest* of the *R* package r*andomForest version 4.5-12* was used. However to build the models further characteristics of random forest needed to be considered. Random forest can show undesirable output classifications when the dependent categorical variables are imbalanced (Chen et al. 2004; Reese et al. 2014). This is due to the fact that random forest seeks to decrease the generalized error. By dealing with imbalanced categorical data it is simple for the random forest algorithm to classify the majority of cases as class which is represented the most and as consequent to reduce the output error (Chen et al. 2004). Furthermore results of Nicodemus (2011) shows that the assessment of variable importance based on the Gini impurity criterion is negatively influenced when random forest is performing with imbalanced categorical data.

These considerations resulted in the present study in down sampling fire severity classes which were highly represented in the training data sets (fire severity class 0 and 3). This down sampling is implemented in the random forest function in *R*. For each classification model integrating metrics derived from post fire aerial images performed in this study the input class composition was altered and the class composition which delivered the most suitable results was chosen. Thereby the main aim was to find a result where all classes are classified with an acceptable accuracy. Furthermore two main settings of the random forest algorithm can be directly influenced by the operator; tuning the amount of trees and tuning the amount of variables used at each split. Therefore for each classification model different settings considering the number of trees (N tree) and the amount of variables (mtry) used at each split was tested in order to seek for model settings where the out of bag generalization error stabilizes on a low level as Boulesteix et al. (2012) suggests. These steps were conducted successively after down sampling the training data sets on an appropriate sample composition considering the four fire severity level. The different tested model settings are displayed in Table 2.

2.3.2 Model creation based on data set (c) including the difference of spectral and spatial metrics derived from both pre and post fire aerial images

Also the independent difference variables computed from pre and post fire aerial images of data set (c) are not following a normal distribution (Shapiro Wilk test; $\alpha = 5\%$) . Furthermore the computed difference variables of data set (c) are correlated to each other. Therefore multicollinearity cannot be excluded. Thus regarding similar considerations as presented for the model creation based on spatial and spectral variables derived from post fire aerial images (see 2.3.2) the random forest algorithm was applied in order to create classification models based on the difference variables computed from spectral and spatial variables derived from pre and post fire aerial images. In total three models were created including either both spectral and spatial difference variables, or only spatial difference variables, or only spectral difference variables. Based on the results of the Wilcoxon signed rank test ($\alpha = 5\%$) it was decided to exclude computed difference variables which altered not significantly after the occurrence of fire. Further different model setting considering the number of trees (N trees) and the number of variables used at each split (mtry) were tested in order to build a model with a low out of bag generalization error. Thereby the same model-setting test approach was conducted as presented for the creation of models based on metrics derived from post fire aerial images. The different tested model settings are displayed in table 2.

Table 2. Tested model settings (number of trees and variables used at each split) of the random forest models integrating either metrics derived from post fire aerial images or difference metrics computed from post and pre fire aerial images

Model metrics derived from post fire aerial images	Model metrics computed from pre and post fire aerial images	N trees	Variables used at each split (mtry)
Spectral and Spatial metrics	Difference spectral and spatial metrics	50, 100, 500, 1000, 2500, 3500, 4500, 5500, 6500, 7500	3, 5, 10, 15, 20
Only spatial metrics	Only difference spatial metrics		3, 5, 10, 15, 20
Only spectral metrics	Only difference spectral metrics		2, 4, 8, 16, 24

2.3.3 Model creation based on data set (d) including metrics derived from post fire Landsat 8 scene

Similar to the independent variables derived from post fire aerial images or computed as a difference of pre and post fire aerial images the independent spectral and thermal variables (data set d) derived and computed from post fire Landsat 8 scene are not normally distributed. Furthermore several variables show a correlation between each other. Therefore similar to the classification based on metrics derived from aerial images the random forest algorithm was considered as classification model. However due to unsatisfying results derived from test runs using the random forest algorithm it was decided to not use random forest. Considering these results ordinal regression more precisely proportional odds logistic regression was used to classify the data. This model is considered as a multivariate extension of the generalized linear model (McCullagh 1980) and the most used regression model considering ordinal data (Bender & Benner 2000). It is further known as the ordinal logistic model (Scott et al. 1997), cumulative odds model (Armstrong & Sloan 1989) and cumulative logit model (Agresti 2010). Agresti (2010) defines the cumulative logit model (proportional odds model) with the following equation.

$$logit\,[P(Y_i \leq j)] = \alpha_j + \beta' x_i$$

For $j = 1, \ldots, c-1$ and where Y is the outcome variable for subject i. x_j denotes a vector of values of independent variables. Whereas β explains the effects of the independent variables and α describes the intercept of each cumulative probability j (Agresti 2010). Due to the fact that two classification models integrate either only NDVI or NBR values computed from spectral metrics derived from the post fire Landsat 8 scene the occurrence of multicollinearity was not expectable. Considering the third computed model based on spectral multicollinearity is probably to occur. Furthermore it was decided to implement only spectral or thermal variables derived from the post fire Landsat 8 scene in the computed classification models with moderate to high correlation coefficients to fire severity. For the computation of the classification models the function *polr* of the package *MASS version 7.3-44* in *R* was used.

2.4 Error analysis and prediction on test data sets

In order to validate the performance of the created classification models each created classification model was applied on a test data set containing 30 % of samples of the original data set as described in the section 2.2.3. These predictions of the different classification models on the test data sets were conducted using the function *predict* of the *R* package *stats version 3.1.0*. Afterwards the results of the predictions more precise the predicted fire severity class membership of each sample of each test data set was compared to the original assessment of fire severity described in section 2.2.3. Thereby confusion matrices were used. These confusion matrices were created using the function *table* of the *R* package *base version 3.1.0.* According to Breiman (2001) the application of random forest models on test data sets is not necessary because the integrated out of bag performance assessment delivers as accurate results as the application of the random forest models on a test data set. However it was decided in the present study to predict all models on test data sets in order to present an independent performance assessment.

Based on the computed confusion matrices the overall accuracy, the user´s accuracy, the producers-accuracy and finally the Cohen's kappa index of each model were calculated. Whereas the overall accuracy was computed by dividing the sum of all correct classifications by the total amount of classified cases times 100. Furthermore the user´s accuracy was computed by dividing the amount of correct classifications of each class by the total count of the class membership derived from the prediction results time 100. The producer´s accuracy of each class was computed by dividing the amount of correct classifications of each class by the total count of class membership derived from the test data sets times 100.

2.4.1 Cohen´s Kappa

Cohen´s Kappa is a widely used method in order to measure classifiers accuracy. It assesses the agreement of two nominal variables considering the cross classification of both variables by integrating the agreement probability due to chance (Ben-David 2008; Warrens 2011). Cohen´s kappa is mathematically defined as:

$$K = \frac{P_0 - P_c}{1 - P_c}$$

Where $P0$ is the agreement probability or accuracy of the classification defined as:

$$p_0 = \sum p_u$$

Where p_u are the correct classification probabilities of each class. Pc is the agreement probability due to chance defined as:

$$P_c = \sum_{i=1}^{I} P(x_i)P(x_j)$$

Where $P(x_i)$ are the column marginal probabilities and $P(x_j)$ are the row marginal probabilities and I is the number of class values (Ben-David 2008). Cohen´s kappa values range on a scale from -1 and 1, whereas high values present a high agreement. Ben-David (2008) considers Cohen´s Kappa simplicity as an advantage in multi-class classifications similar to those created in the present study.

3 Results

3.1 Correlation of variables

In total 98 spectral and spatial variables were extracted from post fire aerial images and considered in the creation of classification models. Among these explanatory variables, 25 variables (all of them spectral variables) show moderate to high correlation coefficients ($Rho \geq 0{,}5$; $Rho \leq -0{,}5$) with fire severity whereas the 95th percentile of the NIR intensity metrics (-0,863) has the highest correlation with fire severity. Thereby high severity classes are represented by low values of the 95th percentile of the NIR intensity metrics and low severity classes with high values of the 95th percentile of the NIR intensity metrics. The calculated correlation coefficients are displayed in table 3 for chosen spectral variables with the highest computed correlation coefficients and all spatial variables. Considering only the extracted spatial variables derived from post fire aerial images the 1st height percentile (-0,425) shows the highest correlation with fire severity, whereas a severity class 0 is represented with high values and fire severity class 3 with low values of the 1st height percentile. The severity classes 1 and 2 do not show a distinct pattern of values of the 1st height percentile. Additionally, without considering the height percentiles, minimum elevation (-0,366) and the percentage of all returns above 2 metres (-0,306) have higher correlations with fire severity than other spatial variables. Also the values of Elev.minimum and values of percentage of all returns above 2 metres show the same pattern like the 1st height percentile; fire severity class 0 is mostly represented by high and fire severity class 3 by low values, the severity classes 1 and 2 don't show a distinct pattern.

Among the 93 difference variables considered in model creation and computed from pre and post fire aerial images 22 variables (all of them spectral variables) show moderate to high correlation coefficients ($Rho \geq 0{,}5$; $Rho \leq -0{,}5$) with fire severity whereas the 90th percentile of the NIR intensity metrics (0,75) has the highest correlation with fire severity, whereas low fire severity classes (0 and 1) are represented by high values and high fire severity classes by low values of the 90th percentile of the NIR intensity metrics The calculated correlation coefficients are displayed in table 4 for chosen spectral variables with the highest correlation coefficients and all spatial variables. Considering only the difference spatial variables computed from pre and post fire aerial images the 1st height percentile (0,346) shows the highest correlation with fire severity, whereas low values of the 1st height percentile are more frequent among fire severity class 0 and high values are more represented among fire severity class 3.

Among the ten spectral metrics derived and computed from satellite images six explanatory variables showed moderate to high ($Rho \geq 0{,}5$; $Rho \leq -0{,}5$) correlations with fire severity, whereas NDVI (-0,865) values and band 5 (NIR) (-0,846) values have the highest correlation with fire severity. Low fire severity classes are represented by high values and high fire severity classes with low values of both metrics. Furthermore NBR shows a high correlation with fire severity (-0,846). The values of NBR regarding fire severity classes show the same pattern like values of band 5 and NDVI. The variables derived or computed from the post fire Landsat 8 scene and their correlation coefficients are displayed in table 5.

Table 3. The highest calculated spearman´s correlation coefficients (Rho) between fire severity and spectral variables derived from post fire aerial images and all calculated spearman´s correlation coefficients (Rho) between fire severity and spatial variables derived from post fire aerial images

Post fire spectral variables	Spearman´s correlation coefficient	Post fire spatial variables	Spearman´s correlation coefficient
NIR.minimum	-0,774	Total.return.count	-0,121
NIR.maximum	-0,786	Elev.minimum	-0,366
NIR d.mean	-0,858	Elev.maximum	-0,235
NIR.stddev	-0,777	Elev.mean	-0,307
NIR.variance	-0,777	Elev.stddev	0,007
NIR.CV	0,085	Elev.variance	0,007
NIR.skewness	0,682	Elev.CV	0,317
NIR.kurtosis	0,644	Elev.skewness	0,155
NIR.P01	-0,773	Elev.kurtosis	0,106
NIR.P05	-0,782	Elev.P01	-0,425
NIR.P10	-0,791	Elev.P05	-0,406
NIR.P20	-0,811	Elev.P10	-0,395
NIR.P25	-0,816	Elev.P20	-0,377
NIR.P30	-0,822	Elev.P25	-0,37
NIR.P40	-0,83	Elev.P30	-0,361
NIR.P50	-0,837	Elev.P40	-0,34
NIR.P60	-0,843	Elev.P50	-0,331
NIR.P70	-0,85	Elev.P60	-0,317
NIR.P75	-0,853	Elev.P70	-0,301
NIR.P80	-0,856	Elev.P75	-0,294
NIR.P90	-0,862	Elev.P80	-0,286
NIR.P95	-0,863	Elev.P90	-0,27
NIR.P99	-0,855	Elev.P95	-0,259
Red.skewness	0,508	Elev.P99	-0,241
Red.kurtosis	0,498	Canopy.relief.ratio	-0,209
Green.skewness	0,544	Percentage.all.returns.above.2.00	-0,341
Green.kurtosis	0,559	All.returns.above.2.00	-0,306
		Percentage.all.returns.above.mean	-0,142
		All.returns.above.mean	-0,183

Table 4. The highest calculated Spearman´s correlation coefficients (Rho) between fire severity and difference spectral variables computed from pre and post fire aerial images and all calculated Spearman´s correlation coefficients (Rho) between fire severity and difference spatial variables computed from pre and post fire aerial images

Spectral difference variables computed from pre and post fire aerial images	Spearman´s correlation coefficient	Spatial difference variables computed from pre and post fire aerial images	Spearman´s correlation coefficient
NIR.minimum	0,632	Total.return.count	0,102
NIR.maximum	0,673	Elev.minimum	0,280
NIR.mean	0,734	Elev.maximum	0,136
NIR.stddev	0,651	Elev.mean	0,272
NIR.variance	0,591	Elev.stddev	0,024
NIR.skewness	-0,653	Elev.variance	-0,002
NIR.kurtosis	-0,634	Elev.CV	-0,210
NIR.P01	0,623	Elev.skewness	-0,126
NIR.P05	0,632	Elev.kurtosis	-0,148
NIR.P10	0,635	Elev.P01	0,346
NIR.P20	0,647	Elev.P05	0,342
NIR.P25	0,654	Elev.P10	0,336
NIR.P30	0,663	Elev.P20	0,325
NIR.P40	0,681	Elev.P25	0,327
NIR.P50	0,701	Elev.P30	0,323
NIR.P60	0,719	Elev.P40	0,313
NIR.P70	0,736	Elev.P50	0,313
NIR.P75	0,742	Elev.P60	0,308
NIR.P80	0,747	Elev.P70	0,298
NIR.P90	0,750	Elev.P75	0,295
NIR.P95	0,743	Elev.P80	0,285
NIR.P99	0,731	Elev.P90	0,260
Red.skewness	-0,462	Elev.P95	0,240
Red.kurtosis	-0,442	Elev.P99	0,183
Green.P50	0,418	Canopy.relief.ratio	0,165
Green.P60	0,444	Percentage.all.returns.above.2.00	0,256
Green.P70	0,451	All.returns.above.2.00	0,293
Green.P75	0,445	All.returns.above.mean	0,171
Green.P80	0,432		

Table 5. Spearman´s coefficient (Rho) between fire severity and spectral and thermal metrics and spectral indices derived or computed from the post fire Landsat 8scene

Landsat 8 post fire scene derived metrics	Spearman´s correlation coefficient
Band 2	0,292
Band 3	-0,324
Band 4	0,329
Band 5	-0,849
Band 6	0,174
Band 7	0,629
Band 10	0,651
Band 11	0,657
NDVI	-0,865
NBR	-0,846

3.2 Model creation

3.2.1 Model based on metrics derived from post fire aerial images

In order to find the most suitable models based on the random forest algorithm integrating metrics derived from post fire aerial images different model settings such as number of trees (N tree), the sample size after down sampling and the number of variables used at each split (mtry) were tested. As a result of this assessment the classification models with the lowest generalization error combined with an appropriate accuracy of each class classification were chosen. The chosen model settings are displayed in table 6. The variables integrated in each model and definitions of these variables can be seen in the appendix. Furthermore the internal assessment of variable importance for each of the post fire aerial derived random forest models is shown in table 7. In the model based on spectral and spatial variables derived from post fire aerial images the 90^{th} percentile of NIR density metrics (mean decrease gini of 27,35) and the 95^{th} percentile of red density metrics (mean decrease gini of 24,03) are identified as the two first most important variables. No spatial variable is among the first 30 most important variables of the model based on spectral and spatial variables derived from aerial images. Considering this model, elev. 80 with a mean decrease gini of 3,46 is identified on rank 31 regarding the internal variable importance assessment of the random forest algorithm. Within the classification model integrating only spatial variables derived from post fire aerial images the independent variable All returns above mean is with a mean decrease gini of 31,47 the most important variable, followed by canopy relief ratio with a mean decrease gini of 30,71. Considering the classification model based on only spectral metrics derived from aerial images the 90^{th} (mean decrease gini = 23,83) and the 80^{th} percentile of NIR density metrics (mean decrease gini = 22,05) are identified by the random forest algorithm as the two first most important variables.

Table 6. Settings of the random forest algorithm for Ntree, sample size and mtry of the classification models including metrics derived from post fire aerial images

Metrics integrated in Random forest model	Ntree	Sample size (Severity class 0,1,2,3)	Mtry
Spectral and spatial metrics	3500	50, 150, 250, 200	15
Only spatial metrics	1000	250, 150, 250, 200	10
Only spectral metrics	2500	150, 150, 150, 150	8

Table 7. Variable importance (mean decrease gini) of the 10 most important metrics of each model based on metrics derived from post fire aerial images

Only spatial metrics derived from post fire aerial images	Mean decrease gini	Spectral and spatial metrics derived from post fire aerial images	Mean decrease gini	Only spectral metrics derived from post fire aerial images	Mean decrease gini
All.returns.above.mean	31,47	NIR.P90	27,35	NIR.P90	23,83
Canopy.relief.ratio	30,71	NIR.P95	24,03	NIR.P80	22,05
Elev.skewness	30,32	NIR.P80	23,18	NIR.P95	21,71
Percentage.all.returns.above.mean	30,24	NIR.stddev	20,87	NIR.mean	20,04
All.returns.above.2.00	29,85	NIR.variance	20,37	NIR.variance	17,97
Elev.kurtosis	29,53	NIR.mean	19,54	NIR.P99	17,95
Elev.P10	28,12	NIR.P75	17,49	NIR.minimum	16,73
Elev.P05	27,35	Red.P75	15,44	NIR.stddev	16,69
Elev.maximum	25,15	NIR.P70	14,14	NIR.P75	15,35
Elev.P01	24,9	NIR.P99	14	NIR.P70	14,36

3.2.2 Model based on difference metrics computed from pre and post fire aerial images

The results of the assessment of different model settings number of trees (N tree), sample size after down sampling and the number of variables used at each split (mtry) of the models integrating computed difference metrics from pre and post fire aerial images are presented in table 8. Based on the pre assessment of the alteration of spatial and spectral metrics derived from aerial images after the occurrence of fire the metrics red mean, 10^{th}, 70^{th}, 75^{th} percentile of red density metrics and the percentage of all returns above mean were not integrated in any model including computed difference metrics of pre and post fire aerial images. This decision was made due to the results of the Wilcoxon signed rank test which showed that the mean ranks of named metrics did not differ between pre and post fire aerial images. Thus it was concluded that these metrics did not alter after occurrence of fire and thus not considered to have a significant impact on the computed classification models considering model performance. The variables integrated in each model can be seen in the appendix. The internal assessment of variable importance for each of the post fire aerial derived random forest models is shown in table 9.

In the model integrating difference spatial and spectral metrics computed from pre and post fire aerial images (data set c), the metric NIR.stddev (mean decrease gini = 18.07) and the 95th percentile of NIR density metrics (mean decrease gini = 15.52) are identified as the most important variables. The first spatial related variable is all returns above 2 metres on rank 17 with a mean decrease gini of 7,8. Considering the model based on the difference of spatial metrics derived from both pre and post fire aerial images percentage of all returns above 2 metres (mean decrease gini = 46,16) is considered to be the most important variable followed by all returns above 2 metres (mean decrease gini = 28,48). In the model based on only difference spectral metrics computed from pre and post fire aerial images the 95th percentile of NIR density metrics (mean decrease gini = 19.01) and the 90th percentile of NIR density metrics (mean decrease gini = 18.17) are considered to be the most important variables.

Table 8. Settings of the random forest algorithm for Ntree, sample size and mtry of the classification models including difference metrics computed from pre and post fire aerial images

Metrics integrated in Random forest model	Ntree	Sample size (Severity class 0,1,2,3)	Mtry
Difference spatial and spectral metrics	3500	50, 150, 250, 200	10
Only difference spatial metrics	2500	150, 150, 150, 150	15
Only difference spectral metrics	500	150, 150, 150, 150	8

Table 9. Variable importance (mean decrease gini) of the 10 most important metrics of each model based on difference metrics computed from pre and post fire aerial images

Difference spatial metrics computed from pre and post fire aerial images	Mean decrease gini	Difference spectral and spatial metrics computed from pre and post fire aerial images	Mean decrease gini	Difference spectral metrics computed from pre and post fire aerial images	Mean decrease gini
Percentage.all.returns.above.2.00	46,17	NIR.stddev	18,07	NIR.P95	19,01
All.returns.above.2.00	28,48	NIR.P95	15,52	NIR.P90	18,17
Elev.mean	23,78	NIR.P90	14,53	NIR.minimum	18,09
All.returns.above.mean	17,41	NIR.P99	14,32	NIR.stddev	17,94
Elev.P25	17,37	NIR.kurtosis	13,16	NIR.P99	17,3
Elev.P01	17,36	NIR.P80	12,87	NIR.CV	16,44
Elev.skewness	17,34	NIR.CV	11,31	NIR.P01	14,51
Elev.P10	16,65	NIR.P75	10,84	NIR.P80	12,52
Canopy.relief.ratio	15,91	Red.P95	15,52	NIR.kurtosis	12,13
Elev.kurtosis	15,87	Red.P90	14,53	NIR.P75	10,36

3.2.3 Model based on metrics derived from post fire Landsat 8 scene

In order to compare the classification models based on metrics derived or computed from aerial images three ordinal regression models integrating either multispectral and thermal metrics (bands 2, 3, 4, 5, 6, 7, 10, 11), the NDVI values or NBR values derived or computed from the post fire Landsat 8 scene were generated.

3.3 Classification accuracy

3.3.1 Internal accuracy assessment of the random forest models

The overall accuracies of the internal performance assessment of the aerial images based random forest models are shown in table 10. Whereby, the model based on only spectral metrics derived from post fire aerial images shows the highest overall accuracy. It is further recognizable that the combination of spectral and spatial variables derived from aerial images improves the overall accuracy of the model compared to the integration of only spatial variables. However the combined model of spectral and spatial variables derived from post fire aerial images does show a similar overall accuracy as the classification model integrating only spectral metrics derived from post fire aerial images. The classification models based on spatial and spectral and based on only spectral difference metrics computed from pre and post fire aerial images show lower OOB overall accuracies as their counterparts based on metrics derived from post fire aerial images. Besides that the classification model based on difference spatial metrics computed from pre and post aerial images shows a higher OOB overall accuracy than its counterpart based on post fire aerial images, yet it is lower than the OOB overall accuracies of the classification models integrating spectral metrics.

Table 10. Out of bag (OOB) overall accuracy of the computed random forest models integrating metrics derived from post fire aerial images and integrating difference metrics computed from pre and post fire aerial images

In data	Post fire aerial images			Difference pre / post fire aerial images		
Metrics	Spatial and spectral	Spatial	Spectral	Spatial and spectral	Spatial	Spectral
OOB overall accuracy	81,83 %	46,43 %	83,10 %	73,42 %	48,86 %	76,28 %

3.3.2 Application of models on test data sets

All classification models were tested on test data sets to assess the performance. The overall accuracy, the producer's accuracy and the user´s accuracy of each tested model are displayed in table 11. In summary it can be seen that in every tested model the user´s accuracy and producer´s accuracy is lowest for fire severity class 1 compared to the calculated user´s and producer´s accuracy of the other fire severity classes within the same model. Furthermore the producer´s accuracies of the fire severity classes 1 and 3 are lower than the producer´s accuracies computed for fire severity classes 0 and 2 in every model based on metrics derived from the post fire Landsat 8 scene. In all other computed models, except in the model integrating difference spatial and spectral metrics computed from pre and post fie aerial images, the producer´s accuracies are highest for fire severity classes 0 and 3. The model integrating only spectral metrics derived from post fire aerial images shows the highest overall accuracy than the other tested models.

Additionally the model integrating only spatial metrics derived from post fire aerial images shows compared to the other tested classification models the lowest overall accuracy, followed by the model integrating only difference spatial metrics computed form pre and post fire aerial images with the second lowest overall accuracy. Furthermore the model integrating only spectral metrics derived from post fire aerial images shows the highest and the model based on only spatial metrics derived from post fire aerial images the lowest computed Cohen´s Kappa value. The computed Cohen´s Kappa values of each model are presented in table 12. The confusion matrix of the best performing model based on spectral metrics derived from aerial images (highest Kappa and overall accuracy) is displayed in table 13.

Table 11. User´s, producer´s and overall accuracy by class of the computed classification models integrating metrics derived from aerial images and the Landsat 8 scene applied on test data sets

User´s accuracy

	In data	Metrics derived from post fire aerial images			Difference metrics computed from post / pre fire aerial images			Metrics and Indices derived and computed from post fire Landsat 8 scene		
Fire severity class	Metric	Spatial and spectral	Spatial	Spectral	Spatial and spectral	Spatial	Spectral	Multispectral / Thermal	NDVI	NBR
0		94,5%	52,1%	93,0%	90,82%	57,71%	88,97%	91,2%	89,3%	87,6%
1		64,8%	20,6%	71,8%	45,92%	32,43%	65,28%	67,3%	62,7%	56,8%
2		80,3%	46,7%	82,3%	70,67%	48,15%	75,65%	67,1%	70,9%	68,7%
3		72,8%	48,6%	74,0%	75,00%	53,06%	67,59%	70,8%	73,6%	64,7%

Producer´s accuracy

	In data	Metrics derived from post fire aerial images			Difference metrics computed from post / pre fire aerial images			Metrics and Indices derived and computed from post fire Landsat 8 scene		
Fire severity class	Metric	Spatial and spectral	Spatial	Spectral	Spatial and spectral	Spatial	Spectral	Multispectral / Thermal	NDVI	NBR
0		80,0%	57,3%	89,3%	59,33%	67,33%	80,67%	91,8%	91,7%	92,4%
1		71,4%	8,3%	72,6%	53,57%	28,57%	55,95%	41,7%	43,2%	33,8%
2		81,6%	49,7%	81,1%	85,95%	42,16%	78,92%	84,8%	85,3%	79,2%
3		83,3%	61,1%	82,2%	73,33%	57,78%	81,11%	54,8%	57,0%	59,1%
	Overall accuracy	79,76%	47,15%	82,32%	70,53%	50,10%	76,03%	74,4%	75,8%	72,7%

Table 12. Cohen´s Kappa values of the computed classification models based on metrics derived from aerial images and the Landsat 8 scene applied on test data set

In data	Metrics derived from post fire aerial images			Difference metrics computed from post / pre fire aerial images			Metrics and Indices derived and computed from post fire Landsat 8 scene		
Metrics	Spatial and spectral	Spatial	Spectral	Spatial and spectral	Spatial	Spectral	Multi-spectral / Thermal	NDVI	NBR
Cohen´s Kappa	0,72	0,26	0,75	0,59	0,31	0,67	0,63	0,65	0,61

Table 13. Confusion matrix of the best performing classification model integrating spectral metrics derived from post fire aerial images applied on test data set

		Reference data				
	Severity class	0	1	2	3	Total
Predicted class	0	**134**	10	1	0	145
	1	11	**61**	10	1	83
	2	3	12	**150**	15	180
	3	2	1	24	**74**	101
	Total	150	84	185	90	**509**
	Overall accuracy (%)	82,32%				

4 Discussion

Comparing the overall accuracies and the calculated Cohen´s Kappa values of all created models, both models including only spatial metrics derived from aerial images or only difference spatial metrics computed from pre and post fire aerial images are ranking lowest. Furthermore the user´s accuracies of each class are lowest for both models including only spatial or only difference spatial metrics compared to the other computed models. A similar result is recognizable considering the producer´s accuracies, whereas there is the exception that the model including spatial metrics derived from only post fire aerial images shows a higher producer´s accuracy of the third fire severity class than the classification models including metrics derived or computed from the post fire Landsat 8 scene. Taking these results into account spatial metrics derived from aerial images extracted by using stereo photogrammetric techniques cannot be seen as a valid alternative to ALS data based approaches as presented by Montealegre et al. (2014) in order to classify forest fire severity. Montealegre et al. (2014) show for 32 ALS data derived spatial metrics moderate to high spearman correlation coefficients to fire severity. Considering that, the present study shows that neither spatial metrics derived from post fire aerial images nor calculated difference spatial metrics computed from pre and post fire aerial images are moderately or highly correlated to fire severity. Furthermore Montealegre et al. (2014) state that the height variable elev.kurtosis shows the strongest correlation with fire severity, whereas in the present study named height metric shows weak correlation with fire severity and ranks low on the internal variable importance assessment of the random forest algorithm of both models integrating only spatial metrics derived from post fire aerial images and the model based on difference metrics computed from pre and post fire aerial images. However by comparing the results of the present study with results of Montealegre et al. (2014) the different methodological approaches need to be considered. Montealegre et al. (2014) divide fire severity only into two classes, low to moderate severity and moderate to high severity, whereas the present study distinguishes between four severity classes. Accordingly it might have been possible that a discrimination between only two fire severity classes in the present study would lead to better classification results of the models integrating only spatial metrics derived from post fire aerial images and integrating difference metrics computed from pre and post fire aerial images. This interpretation is further supported by the fact that the producer´s accuracies of all models integrating metrics derived or computed from aerial images, except for the model integrating difference spectral and spatial metrics computed from pre and post fire aerial images, are highest for the fire severity classes on the ends of the ordinal fire severity class scale (class 1 and 3). Furthermore the present study relies on fire severity assessment of Nilsson et al. (2014) which is based on the remote assessment of tree crown damage, whereas Montealegre et al. (2014) base their classification on in field fire severity assessment using CBI, which is a subjective estimation of averaged fire severity across 5 forest strata, such as substrate, herbal vegetation, large shrubs, small and intermediate tress and dominant canopy trees. However due the fact that DSM created by image matching techniques do not penetrate the canopy in the way that DSM based on ALS data do, an infield assessment of fire severity of lower forest strata (substrate, herbal vegetation, shrubs and small trees) was not considered to be of any advantage regarding model performance in the present study.

Nevertheless the fact that the stereo photogrammetric technique does not penetrate the forest canopy might be a reason for the poor performance of the models integrating either spatial metrics derived from post fire aerial images or difference spatial metrics computed from pre and post fire aerial images.

Considering the overall accuracy and Cohen´s Kappa values of the models including either spatial and spectral metrics derived from post fire aerial images or including difference spatial and spectral metrics computed from pre and post fire aerial images, moderate to substantial classification results are recognizable. Whereas, the overall classification accuracy of the model integrating spatial and spectral metrics derived from post fire aerial images is nearly as high as the overall accuracy of the model based on spectral metrics derived from post fire aerial images. However the good results are most probably not due to the combination of both spatial and spectral metrics, but mainly due to the impact of spectral metrics on named models. This is justifiable by the fact that in both models integrating either spatial and spectral metrics derived from post fire aerial images or difference spatial and spectral metrics computed from pre and post fire aerial images, the included spatial variables rank on low ranks considering the internal assessment of variable importance of the random forest algorithm.

Both models integrating either difference spatial and spectral metrics or only difference spectral metrics computed from pre and post fire aerial images show lower overall accuracies and Cohen´s Kappa values than the models based on either spatial and spectral metrics or only spectral metrics derived from post fire aerial images. These results show that additional information in form of metrics derived from pre fire aerial images does not increase the performance of the classification models. Besides that the combination of spatial metrics derived from pre and post fire aerial images resulted in an increased overall accuracy and Cohen´s Kappa value compared to the model integrating only spatial metrics derived from post fire aerial images. However the model integrating difference metrics computed from pre and post fire aerial images still shows undesirable model performance.

In contrast a good performance of the classification model integrating spectral metrics derived from post fire aerial images, which shows the highest overall accuracy and Cohen´s Kappa value of all computed models, is assessed in the present study. Due to the fact that spectral metrics derived from satellite images are already in use in order to classify fire severity (Chafer et al. 2004; Epting et al. 2005; Escuin et al. 2008; French et al. 2008; Hoy et al. 2008; Keeley et al. 2008; Miller & Yool 2002), a good performance of named model was expectable. However it was unexpected that the model integrating spectral metrics derived from post fire aerial images shows a better performance than the generated models integrating metrics derived and computed from the post fire Landsat 8 scene. This might be due to the fact that the post fire aerial images have in contrast to the post fire Landsat 8 scene a smaller ground sampling distance. Thus each sample plot is described by many pixels in the post fire aerial images, which increases the spectral information used to classify fire severity and thus the performance of the classifier. Whereby, in the post fire Landsat 8 scene each sample plot is covered by only one pixel.

Another reason for the better performance of the model integrating spectral metrics derived from post fire aerial images compared with the models based on metrics derived or computed from the Landsat 8 scene might be due to different image characteristics of the Landsat 8 scene and the aerial images in combination with the fact the infield fire severity assessment on plot level was conducted by the interpretation of tree canopy damages. The used aerial images show a higher proportion of tree canopies than the Landsat 8 scene due to higher average incidence angles. Thus the aerial images carry more information about the tree canopy which are directly relatable to the infield fire severity assessment than the Landsat 8 scene. This affect that more information of the tree canopy and less information of terrain affect the performance of the model based on only spectral metrics derived from aerial images is further enhanced by the used method of extracting the spectral metrics from the generated 3D point clouds of the forest canopy.

In comparison to the results of Epting et al. (2005) the best performing model of the present study namely the model integrating only spectral metrics derived from post fire aerial images, shows a higher overall accuracy and a higher Cohen´s Kappa value than the classification models computed by Epting et al. (2005).

The highest overall accuracy (80,77 %) and Cohen´s Kappa value (0.64) computed by Epting et al. (2005) is shown by a model integrating single date NBR values computed from Landsat TM and ETM+ images describing three fire severity classes and including only forested areas. However in comparison to the results of Chafer et al. (2004) the model integrating only spectral metrics derived from post fire aerial images computed in the present study shows a slightly lower overall accuracy. Chafer et al. (2004) investigate fire severity of wildfires in the greater Sydney Basin Australia in 2001 by using NDVI and dNDVI computed from pre and post fire SPOT2 images and calculated a high overall accuracy (88%) and Kappa values for each of 6 fire severity classes above 0.8 for a classification model integrating dNDVI metrics. However while comparing the performance of the model integrating only spectral metrics derived from post fire aerial images with the results of other studies the differences in the applied methods need to be considered. Nevertheless it is appropriate to summarize that the best performing model computed by the present study delivers similar good or even better results than models created by named other studies.

Differently to the studies of Epting et al. (2005), Escuin et al. (2008) and Hoy et al. (2008) the results of the present study indicate that the NDVI variable derived from the post fire Landsat 8 scene is slightly stronger correlated to forest fire severity than the NBR variable. However both models based on either NDVI or NBR metrics computed from the post fire Landsat 8 scene show substantial overall accuracies and Cohen´s Kappa values corroborating the results of (Epting et al. 2005; Escuin et al. 2008). Besides that the model based on spectral and thermal metrics derived from the post fire Landsat 8 scene shows also a substantial overall accuracy and Cohen´s Kappa value. This result is consistent with the result of Michalek et al. (2000) who used Landsat TM bands 1 -5 and 7 to estimate carbon release from a fire in an Alaskan spruce forest. Besides the overall good model performance of Landsat 8 metric based classification models the fact that the producer´s accuracies of the three models are lowest for fire severity classes 1 and 3 is noticeable.

In the present study particularly the spectral bands 5 and 7 and the thermal bands 10 and 11 are strongly correlated with fire severity. The fact that Band 5 and 7 is strongly correlated to fire severity is already considered and implemented in the NBR Index. However the correlation of the thermal bands 10 and 11 is not often recognized due to the fact that thermal metrics derived from satellite images were not focused in past studies (Epting et al. 2005). Nevertheless similar to the results of the present study high correlations of the thermal bands of Landsat TM/ETM+ with fire severity are indicated by Epting et al. (2005).

Besides the discussion of the results it is further to discuss whether the term fire severity is applied according to its definition as it relates basically to the loss of biomass above and below ground (Keeley 2009). Due to the fact that in the present study the severity assessment of Nilsson et al. (2014) is used which is relating to the damage of tree crowns due to fire, it is reasonable to use the term fire severity in this context. However it needs to be considered as stated above and by Keeley (2009) that the term itself is used very heterogeneously and several other studies consider also damages of the ground e.g. in the assessment of forest fire severity by using the CBI assessment (Epting et al. 2005; Escuin et al. 2008; Allen & Sorbel 2008; Montealegre et al. 2014). Furthermore the accuracy and performance of the results presented in this study might be affected by intrinsic errors of the used methods. One main source of errors is based in the generation of the DSM using image matching, namely SGM. In general image matching techniques are challenged by several environmental and technical problems (Baltsavias et al. 2008).

These problems are for instance little or no texture, moving objects, occlusions and illumination conditions (Baltsavias et al. 2008). Particularly the multi temporal approaches presented in this study might be affected by additionally difficulties, such as different image qualities and illumination characteristics due to different times of image recording (Baltsavias et al. 2008). Additionally regarding the performance of aerial image based models presented in this study the low overlap (60 % along flight strips and 30 % across strips) of the used aerial images might be another source for errors. Considering the findings of Hirschmüller & Bucher (2010) regarding the evaluation of DSM a low overlap of aerial images may cause problems particularly in forests or streets, due to large view angels. They propose to use an overlap of 80 % along flight strips and 70 % across strips. However a higher overlap automatically results in increased flight costs (Haala 2009). Additionally the models based on metrics derived or computed from the post fire Landsat 8 scene can be affected by errors associated by the Landsat 8 scene. Those errors can occur due to the sensor calibration and resolution, orbital and sensor degradation, ground and atmospheric conditions and digital quantization errors (Pettorelli et al. 2005; Escuin et al. 2008). Furthermore it needs to be considered that only short term effects of fire on the vegetation are described by the computed classification models due to the fact that the post fire Landsat 8 scene and post fire aerial images were acquired directly after the occurrence of fire. However White et al. (1996) concludes that mapping of fire characteristics should be conducted soon after the occurrence of fire, due to the fact that re-growing vegetation has a negative effect on the detection of fire perimeters (Cocke et al. 2005). A further error affecting the performance of the calculated models might be immanence in the remote fire severity assessment on sample plot level of Nilsson et al. (2014).

This study shows that the use of spatial metrics derived from either post fire aerial images or difference spatial metrics computed from pre and post fire aerial images leads to poor results in order to classify and map forest fire severity. Furthermore models integrating thermal and spectral metrics derived from the post fire Landsat 8 scene or indices derived from the post fire Landsat 8 scene show substantial performance results. A combination of metrics derived from pre and post fire aerial images does not increase model performance. Nevertheless the highest model performance is shown by the model integrating only spectral metrics derived from post fire aerial images.

5 Outlook future research

Considering the results of the present study it might not be of interest for future research to focus further on fire severity classification using spatial metrics derived from aerial images using stereo photogrammetric techniques. However if it is desired to further analyze the application of stereo photogrammetry in order to classify forest fire severity, it might be interesting to use different stereo photogrammetric techniques, or different technical settings considering the acquisition of aerial images. Accordingly it might be of advantage to increase the overlap of the aerial images or to use post fire aerial images acquired after a longer period than used in the present study, in order to analyze whether a longer vegetation response period has an effect on the derived spatial metrics. Furthermore it might be of interest to investigate whether the classification approach based on stereo photogrammetric aerial image matching will deliver similar results in different environmental conditions than investigated in the present study. Furthermore it can be stressed that the use of spectral metrics derived from aerial images seems to be a promising approach for future applications of forest fire severity classification, especially considering the results of Montealegre et al. (2014) a combination of ALS data and spectral data derived from aerial images might deliver good results. Besides that the results of the present study in combination with the considerations of Epting et al. (2005) reveal a possibility to use thermal metrics in order to classify fire severity in future studies. Furthermore it shall be stressed that it is desirable to create an overall accepted definition of forest fire severity and a globally applied approach to assess fire severity on site. Thus it would be easier to compare different remote sensing techniques in order to classify forest fire severity.

References

Agresti, A. (2010) Analysis of Ordinal Categorical Data. John Wiley & Sons, Inc, Hoboken,New Jersey, USA, 47 - 49.

Allen, J. L. & Sorbel, B. (2008) Assessing the differenced Normalized Burn Ratio's ability to map burn severity in the boreal forest and tundra ecosystems of Alaska's national parks. *International Journal of Wildland Fire*, 17(4), 463–475.

Angelstam, P. K. (1998) Maintaining and Restoring Biodiversity in European Boreal Forests by Developing Natural Disturbance Regimes. *Journal of Vegetation Science*, 9(4), pp.593–602.

Armstrong, B. G. & Sloan, M. (1989) Ordinal regression models for epidemiologic data. *Am J Epidemiol*, 129(1), 191–204.

Baltsavias, E. (1999) A comparision between photogrammetry and laser scanning. ISPRS Journal of Photogrammetry and Remote Sensing, 54(2-3), 83–94.

Baltsavias, E., Gruen, A., Eisenbeiss, H., Zhang, L., & Wasser, L., T. (2008). Highquality image matching and automated generation of 3D tree models. *International Journal of Remote Sensing*, 29(5), 1243–1259.

Ben-David, A. (2008) About the relationship between ROC curves and Cohen's kappa. Engineering Applications of Artificial Intelligence, 21(6), 874–882.

Bender, R. & Benner, A. (2000) Calculating Ordinal Regression Models in SAS and S-Plus. Biometrical Journal, 42(6), 677–699.

Bergeron, Y., Leduc, A., Harvey, B. D. & Gauthier S. (2002) Natural Fire Regim: A Guide for Sustainable Management of the Canadian Boreal Fores. *Silva Fennica*, 36(1), 81–95.

Bohlin, J., Wallerman, J. & Fransson, J. E. S. (2012). Forest variable estimation using photogrammetric matching of digital aerial images in combination with a high-resolution DEM. *Scandinavian Journal of Forest Research*, 27(7), 692–699.

Boulesteix, A. L., Janitza, S., Kruppa, J. & König, I. R. (2012) Overview of Random Forest Methodology and Practical Guidance with Emphasis on Computational Biology and Bioinformatics. (129).

Breiman, L. (2001) Random forests. *Machine learning*, 45(1),5–32.

Burton, P. J., Parisien, M. A., Hicke, J. A., Hall, R. J. & Freeburn, J. T. (2008) Large fires as agents of ecological diversity in the North American boreal forest. *International Journal of Wildland Fire*, 17(6), 754–767.

Chafer, C. J., Noonan, M. & Macnaught, E. (2004) The post-fire measurement of fire severity and intensity in the Christmas 2001 Sydney wildfires. *International Journal of Wildland Fire*, 13(2), 227–240.

Chapin, F. S. et al. (2006) Sucessional Processes in the Alaskan Boreal Forest. In Chapin, F. S., Oswood, M. W., Cleve, K. V., Viereck, L. A., Verbyla, D. L., (Eds.) Alaska's Changing Boreal Forest, Oxford University Press, Inc., New York.Chen, C., Liaw, A. & Breiman, L. (2004) Using random forest to learn imbalanced data. *unpublished technical report*, 1–12.

Chuvieco, E., Mart, M. P. & Palacios, A. (2002) Assessment of different spectral indices in the red–near-infrared spectral domain for burned land discrimination. *Int. J. Remote Sensing*, 23(23), 5103–5110. 33

Cocke, A. E., Fulé, P. Z. & Crouse, J.E. (2005) Comparison of burn severity assessments using Differenced Normalized Burn Ratio and ground data. *International Journal of Wildland Fire*, 14(2), 189.

Conard, S. G., Sukhinin A. I., Stocks, B. J., Cahoon, D. R., Davidenko, E. P. and Ivanova, G. A. (2002) on Carbon Cycling and Emissions in Siberia. *Climatic Change*, 197–211.

Dahlberg, A., Schimmel, J., Taylor, A. F. S. & Johannesson, H. (2001) Post-fire legacy of ectomycorrhizal fungal communities in the Swedish boreal forest in relation to fire severity and logging intensity. *Biological Conservation*, 100(2), 151–161.

Díaz-Uriarte, R. & Alvarez de Andrés, S. (2006) Gene selection and classification of microarray data using random forest. *BMC bioinformatics*, 7, 3.

Epting, J., Verbyla, D. & Sorbel, B. (2005) Evaluation of remotely sensed indices for assessing burn severity in interior Alaska using Landsat TM and ETM+. *Remote Sensing of Environment*, 96(3-4), 328–339.

Escuin, S., Navarro, R. & Fernández, P. (2008) Fire severity assessment by using NBR (Normalized Burn Ratio) and NDVI (Normalized Difference Vegetation Index) derived from LANDSAT TM/ETM images. *International Journal of Remote Sensing*, 29(4), 1053–1073.

Esseen, A. P., Ehnström, B., Ericson, L. & Sjöberg, K. (1997) Oikos Editorial Office Boreal Forests Boreal. , (46), 16–47.

French, N. H. F, Kasischke, E. S., Hall, R. J., Murphy, K. A., Verbyla, D. L., Hoy, E. E. & Allen, J. L. (2008). Using Landsat data to assess fire and burn severity in the North American boreal forest region: an overview and summary of results. *International Journal of Wildland Fire*, 17, 443–462.

Gehrke, S., Morin, K., Downey, M., Boehrer, N. & Fuchs, T. (2008) Semi-global matching: an alternative to lidar for dsm generation? International Archives of the Photogrammetry, Remote Sensing and Spatial Information Sciences, XXXVIII-B1, 1–6.

Gislason, P.O., Benediktsson, J.A. & Sveinsson, J.R. (2006) Random forests for land cover classification. *Pattern Recognition Letters*, 27(4), 294–300.

Gobakken, T., Bollandsås, O.M. & Næsset, E. (2015) Comparing biophysical forest characteristics estimated from photogrammetric matching of aerial images and airborne laser scanning data. *Scandinavian Journal of Forest Research*, 30(1), 73–86.

Grafström, A. (2016). BalancedSampling: Balanced and Spatially Balanced Sampling. R package version 1.5.1. http://www.antongrafstrom.se/balancedsampling

Granström, A. (1993) Spatial and temporal variation in lightning inginitions in Sweden. *Journal of* Vegetation Science, 4(6), 737–744.

H. Hirschmüller, H. (2008) Accurate and efficient stereo processing by semi-global matching and mutual information. IEEE International Conference on Computer Vision and Pattern Recognition, 2(2), 807–814.

Haala, N. (2009) Comeback of Digital Image Matching. *Photogrammetric Week 2009*, 289–301.

Haala, N., Hastedt, H., Wolf, K., Ressl, M., & Baltrusch, S. (2010) Digital Photogrammetric Camera Evaluation - Generation of digital elevation models. PFG. 2010(2), 99-115.

Hammill, K. A., & Bradstock, R., A. (2006) Remote sensing of fire sensitivity in the Blue Mountains: influence of vegetation type and inferring fire intensity. *International Journal of Wildland Fire*, 15, 213–226. 34

Hapfelmeier, A., Hothorn, T., Ulm, K. & Strobl, C. (2014) A new variable importance measure for random forests with missing data. *Statistics and Computing*, 24(1), 21–34.

Heurich, M., Schadeck, S., Weinacker, H. & Krzystek, P. (2003) Forest Parameter Deriviation from DTM / DSM generated from LIDAR and Digital Modular Camera (DMC). *XX ISPRS Congress. Istanbul, Turkey*.

Hirschmüller, H. & Bucher, T. (2010) Evaluation of digital surface models by semi-global matching. DGPF Tagungsband.

Hoy, E. E., French, N. H. F., Turetsky, M. R., Trigg, S. N. & Kasischke E. S. (2008) Evaluating the potential of Landsat TM/ETM+ imagery for assessing fire severity in Alaskan black spruce forests. *International Journal of Wildland Fire*, 17(4), 500–514.

Huete, A. R. (1988) A Soil-Adjusted Vegetation Index (SAVI). *Remote Sensing of Environment*, 25, 295-309.

Järnstedt, J., Pekkarinen, A., Tuominen, S., Ginzler, C., Holopainen, M. & Viitala, R. (2012) Forest variable estimation using a high-resolution digital surface model. *ISPRS Journal of Photogrammetry and Remote Sensing*, 74, 78–84.

Keeley, J. E. (2009) Fire intensity, fire severity and burn severity: A brief review and suggested usage. International Journal of Wildland Fire, 18(1), 116–126.

Keeley, J. E., Brennan, T. & Pfaff, A., H. (2008) Fire Severity and Ecosytem Responses Following Crown Fires in California Shrublands. *Ecological Applications*, 18(6), 1530–1546.

Lentile, L. B., Holden, Z. A., Smith, A. M. S., Falkowski, M. J., Hudak, A. T., Morgan, P., Lewis, S. A., Gessler, P. E. & Benson, N. C. (2006) Remote sensing techniques to assess active fire characteristics and post fire effects. *USDA Forest Service / UNL Faculty Publications*, 194(5), 319-345.

McCullagh, P. (1980) Regression Models for Ordinal Data. *Journal of the Royal Statistical Society*, 42(2), 1–22.

McGaughey, R. J. (2014) FUSION/LDV: Software for LIDAR Data Analysis and Visualization, March 2014 – FUSION Version 3.42. Manual. United States Department of Agriculture, Forest Service, Pacific Northwest Research Station.

Michalek, J. L., French, N. H. F., Kasischke, E. S., Johnson, R. D. & Colwell, J. E. (2000) Using Landsat TM data to estimate carbon release from burned biomass in an Alaskan spruce forest complex. *International Journal of Remote Sensing*, 21(2), 323–338.

Miller, J. D. & Yool, S. R. (2002) Mapping forest post-fire canopy consumption in several overstory types using multi-temporal Landsat TM and ETM data. *Remote Sensing of Environment*, 82(2-3), 481–496.

Montealegre, A. L., Lamelas, M. T., Tanase, M. A. & de la Riva, J. (2014) Forest fire severity assessment using ALS data in a mediterranean environment. *Remote Sensing*, 6(5), 4240–4265.

Morgan, P., Hardy, C. C., Swetnam, T. W., Rollins, M. G. & Long, D. G. (2001) Mapping fire regimes across time and space: Understanding coarse and fine-scale fire patterns. *International Journal of Wildland Fire*, 10(4), 329–342.

Næsset, E. (2002) Determination of Mean Tree Height of Forest Stands by Digital Photogrammetry. Scandinavian Journal of Forest Research, 17(5), 446–459.

Nicodemus, K. K. (2011) Letter to the editor: on the stability and ranking of predictors from random forest variable importance measures. *Briefings in bioinformatics*, 12(4), 369–73.

Nilsson, B., Tyboni, M., Pettersson, A., Granström, A. & Olsson, H. (2014) Punktgittertolkning av brandområdet i Västmanland. Redovisning av uppdrag från Skogsstyrelsen. Unpublished report. Institutionen för skoglig resurshushållning. Sveriges Lantbruksuniversitet, Umeå.

Pal, M. (2005) Random forest classifier for remote sensing classification. *International Journal of Remote Sensing*, 26(1), 217–222. 35
Pettorelli, N., Vik, J. O., Mysterud, A., Gaillard, J. M., Tucker, C. J. & Stenseth, N. C. (2005) Using the satellite-derived NDVI to assess ecological responses to environmental change. *Trends in Ecology and Evolution*, 20(9), 503–510.
Pinty, B. & Verstraete, M. M. (1992) GEMI: a non-linear index to monitor global vegetation from satellites. *Vegetatio*, 101, 15-20.
Quinlan, J. (1993) C4. 5: programs for machine learning. *Machine Learning*, 240, 302.
Rees, D. C. & Juday, G. P. (2002) Plant species diversity and forest structure on logged and burned sites in central Alaska. *Forest Ecology and Management*, 155, 291 – 302.
Reese, H., Nyström, M., Nordkvist, K. & Olsson, H. (2014) Combining airborne laser scanning data and optical satellite data for classification of alpine vegetation. *International Journal of Applied Earth Observation and Geoinformation*, 27, 81–90.
Reitinger, B., Sormann, M., Zebedin, L., Schachinger, B., Hoefler, M., Tomasi, R., Lamperter, M., Gruber, B., Schiester, G., Kobald, M., Unger, M., Klaus, A., Bernoegger, S., Karner, K., Wichert, A., Ponticelli, M., Gruber, M. (2012) Ultramap V3 – A Revolution In Aerial Photogrammetry. International Archives of the Photogrammetry, Remote Sensing and Spatial Information Sciences, Volume XXXIX-B4, 2012 XXII ISPRS Congress, 25 August – 01 September 2012, Melbourne, Australia.
Rodriguez-Galiano, V. F., Ghimire, B., Rogan, J., Chica-Olmo, M. & Rigol-Sanchez, J. P. (2012) An assessment of the effectiveness of a random forest classifier for land-cover classification. *ISPRS Journal of Photogrammetry and Remote Sensing*, 67(1), 93–104.
Rogan, J. & Franklin, J. (2001) Mapping Wildfire Burn Severity in Southern California Forests and Shrublands Using Enhanced Thematic Mapper Imagery. *Geocarto International*, 16(4), 91–106.
Rothermel, M. & Haala, N. (2011) Potential of Dense Matching for the Generation of High Quality Digital Elevation Models. International Society for Photogrammetry and Remote Sensing, XXXVII(4-W19), 14–17.
Roy, D. P., Boschetti, L. & Trigg, S. N. (2006) Remote sensing of fire severity: Assessing the performance of the normalized burn ratio. *IEEE Geoscience and Remote Sensing Letters*, 3(1), 112–116.
Schimmel, J. & Granström, A. (1996) Fire severity and vegetation response in the boreal Swedish forest. *Ecology*, 77(5), 1436–1450.
Scott, S. C., Goldberg, M. S. & Mayo, N. E. (1997) Statistical assessment of ordinal outcomes in comparative studies. *Journal of Clinical Epidemiology*, 50(1), 45–55.
Stocks, B. J., Forsberg, M. A., Lynham, T. J., Mearns, L., Wotton, B. M., Yang, Q., Jin, J. Z., Lawrence, K., Hartley, G. R., MAson, J. A. & McKenney, D. W. (1998) Climate change and forest fire potential in Russian and Canadian boreal forests. *Climatic Change*, 38(1), 1–13.
Suffling, R., Lihou, C. & Morand, Y. (1988) Control of landscape diversity by catastrophic disturbance: a theory and a case study of fire in a canadian boreal forest. *Environmental Management*, 12(1), 73–78.
Tirén, L. 1937: Forestry historical studies in the Degerfors district of the province of Västerbotten. Medd. Stat. Skogsförs. Anst. 30: 67-322, in Swedish with English summary.
Warrens, M. J. (2011) Cohen's quadratically weighted kappa is higher than linearly weighted

kappa for tridiagonal agreement tables. *Statistical Methodology*, 9(3), 440–444.
Wiechert, A., Gruber, M. (2011) UltraCam and UltraMap – Towards All in One Solution by Photogrammetrie. In Fritsch, D. (2011) Photogrammetric Week `11. Wichmann/VDE Verlag, Berlin Offenbach.
Verbyla, D. L., Kasischke, E. S. & Hoy, E. E. (2008) Seasonal and topographic effects on estimating fire severity from Landsat TM/ETM+ data. *International Journal of Wildland Fire*, 17(4), 527–534.
White, J. D., Ryan, K. C., Key, C. C. & Running, S. W. (1996) Remote Sensing of Forest Fire Severity and Vegetation Recovery. 6(3), 125–136.
Wikars, L. & Schimmel, J. (2001) Immediate effects of ® re-severity on soil invertebrates in cut and uncut pine forests. *Forest Ecology and Management*, 141, 189–200. 36
Viola, P. & Wells, W. M.. I. (1995) Alignment by maximization of mutual information. Proceedings of IEEE International Conference on Computer Vision, 24(2), 16–23.
Wotton, B. M., Nock, C. A. & Flannigan, M. D. (2010) Forest fire occurrence and climate change in Canada. International Journal of Wildland Fire, 19(3), 253–271.
Zackrisson, O. (1977) Influence of forest fires on the North Swedish boreal forest. *Oikos*, 29(1977), 22–32.

Appendix

Equations of vegetation indexes present in the introduction

The **BAI** is defined as following:

$$\text{BAI} = \frac{1}{((pc_r - p_r)^2 + (pc_{nir} - p_{nir})^2)}$$

where p_r and p_{nir} are the pixel reflectance of red and near infrared and p_r and p_r the reference reflectance of the red and near infrared (Chuvieco 2002).

The **SAVI** is defined by Huete (1988) as following:

$$\text{SAVI} = \frac{(NIR - red)}{(NIR + red + L)} \times (1 + L)$$

Where L is a constant considering the graphical adjustment of the spectral vegetation reflectance isolinesr.

The **GEMI** is defined as following:

$$GEMI = n\,(1 - 0.25 \times n) - \frac{(p_1 - 0.125)}{(1 - p_1)}$$

where

$$n = \frac{2 \times ((p_2{}^2 - p_1{}^2) + 1.5 \times p_2 + 0.5 \times p_1)}{(p_2 + p_1 + 0.5)}$$

and p_1 is the reflectance of the near infrared spectral region and p_1 is the reflectance of the red spectral region Pinty & Verstraete (1992).

Table. 1. Computed and tested model approaches in order classify forest fire severity of the forest fire in Västmanland (Central Sweden)

	Approach 1	Approach 2	Approach 3	Approach 4	Approach 5	Approach 6	Approach 7	Approach 8	Approach 9
Multispectral metrics derived from post fire aerial images	x		x						
Spatial metrics derived from post fire aerial images		x	x						
Difference of spatial metrics derived from post fire and pre fire aerial images				x		x			
Difference of spectral metrics derived from post fire and pre fire aerial images					x	x			
Multispectral and thermal metrics derived from post fire Landsat 8 scene							x		
NDVI metrics computed from post fire Landsat 8 scene								x	
NBR metrics computed from post fire Landsat 8 scene									x

Metrics derived from pre and post fire aerial images

A definition of all metrics computed by *FUSION* is summarized by McGaughey (2014). In the following there is a list of definitions of metrics presented in this study which are in need of further description in order to help understanding the presented results.

Table. 2. Definition of FUSION computed metrics in need of further description

Metric generated by *FUSION*	Definition by McGaughey (2014)
Elev.	Elevation
NIR.	Near Infrared
.stddev	Standard deviation
.P01,.P05,.P010,.P20,.P25,.P30,.P40,.P50,.P60,.P70,.P75,.P80,.P90,.P95,.P99	Percentile values
.CV	Coefficient of variation
Canopy.relief.ratio	((mean – min) / (max – min))

Table. 3. All metrics computed from post fire aerial images integrated in fire severity classification models

Only spatial metrics derived from post fire aerial images	Spectral and spatial metrics derived from post fire aerial images	only spectral metrics derived from post fire aerial images
Elev.minimum	NIR.minimum	NIR.minimum
Elev.maximum	NIR.maximum	NIR.maximum
Elev.mean	NIR.mean	NIR.mean
Elev.stddev	NIR.stddev	NIR.stddev
Elev.variance	NIR.variance	NIR.variance
Elev.CV	NIR.CV	NIR.CV
Elev.skewness	NIR.skewness	NIR.skewness
Elev.kurtosis	NIR.kurtosis	NIR.kurtosis
Elev.P01	NIR.P01	NIR.P01
Elev.P05	NIR.P05	NIR.P05
Elev.P10	NIR.P10	NIR.P10
Elev.P20	NIR.P20	NIR.P20
Elev.P25	NIR.P25	NIR.P25
Elev.P30	NIR.P30	NIR.P30
Elev.P40	NIR.P40	NIR.P40
Elev.P50	NIR.P50	NIR.P50
Elev.P60	NIR.P60	NIR.P60
Elev.P70	NIR.P70	NIR.P70
Elev.P75	NIR.P75	NIR.P75
Elev.P80	NIR.P80	NIR.P80
Elev.P90	NIR.P90	NIR.P90
Elev.P95	NIR.P95	NIR.P95
Elev.P99	NIR.P99	NIR.P99
Canopy.relief.ratio	Red.minimum	Red.minimum
Percentage.all.returns.above.2.00	Red.maximum	Red.maximum
All.returns.above.2.00	Red.mean	Red.mean
Percentage.all.returns.above.mean	Red.stddev	Red.stddev
All.returns.above.mean	Red.variance	Red.variance
	Red.CV	Red.CV
	Red.skewness	Red.skewness
	Red.kurtosis	Red.kurtosis
	Red.P01	Red.P01

	spectral and spatial metrics derived from post fire aerial images	only spectral metrics derived from post fire aerial images
	Red.P05	Red.P05
	Red.P10	Red.P10
	Red.P20	Red.P20
	Red.P25	Red.P25
	Red.P30	Red.P30
	Red.P40	Red.P40
	Red.P50	Red.P50
	Red.P60	Red.P60
	Red.P70	Red.P70
	Red.P75	Red.P75
	Red.P80	Red.P80
	Red.P90	Red.P90
	Red.P95	Red.P95
	Red.P99	Red.P99
	Green.minimum	Green.minimum
	Green.maximum	Green.maximum
	Green.mean	Green.mean
	Green.stddev	Green.stddev
	Green.variance	Green.variance
	Green.CV	Green.CV
	Green.skewness	Green.skewness
	Green.kurtosis	Green.kurtosis
	Green.P01	Green.P01
	Green.P05	Green.P05
	Green.P10	Green.P10
	Green.P20	Green.P20
	Green.P25	Green.P25
	Green.P30	Green.P30
	Green.P40	Green.P40
	Green.P50	Green.P50
	Green.P60	Green.P60
	Green.P70	Green.P70
	Green.P75	Green.P75
	Green.P80	Green.P80
	Green.P90	Green.P90
	Green.P95	Green.P95
	Green.P99	Green.P99
	Elev.minimum	

	spectral and spatial metrics derived from post fire aerial images
	Elev.maximum
	Elev.mean
	Elev.stddev
	Elev.variance
	Elev.CV
	Elev.skewness
	Elev.kurtosis
	Elev.P01
	Elev.P05
	Elev.P10
	Elev.P20
	Elev.P25
	Elev.P30
	Elev.P40
	Elev.P50
	Elev.P60
	Elev.P70
	Elev.P75
	Elev.P80
	Elev.P90
	Elev.P95
	Elev.P99
	Canopy.relief.ratio
	Percentage.all.returns.above.2.00
	All.returns.above.2.00
	Percentage.all.returns.above.mean
	All.returns.above.mean
	Total.return.count

Table. 4. All difference metrics computed from pre and post fire aerial images integrated in fire severity classification models

Only difference spatial metrics computed from pre and post fire aerial images	Difference spectral and spatial metrics computed from pre and post fire aerial images	Only difference spectral metrics computed from pre and post fire aerial images
Elev.minimum	NIR.minimum	NIR.minimum
Elev.maximum	NIR.maximum	NIR.maximum
Elev.mean	NIR.mean	NIR.mean
Elev.stddev	NIR.stddev	NIR.stddev
Elev.variance	NIR.variance	NIR.variance
Elev.CV	NIR.CV	NIR.CV
Elev.skewness	NIR.skewness	NIR.skewness
Elev.kurtosis	NIR.kurtosis	NIR.kurtosis
Elev.P01	NIR.P01	NIR.P01
Elev.P05	NIR.P05	NIR.P05
Elev.P10	NIR.P10	NIR.P10
Elev.P20	NIR.P20	NIR.P20
Elev.P25	NIR.P25	NIR.P25
Elev.P30	NIR.P30	NIR.P30
Elev.P40	NIR.P40	NIR.P40
Elev.P50	NIR.P50	NIR.P50
Elev.P60	NIR.P60	NIR.P60
Elev.P70	NIR.P70	NIR.P70
Elev.P75	NIR.P75	NIR.P75
Elev.P80	NIR.P80	NIR.P80
Elev.P90	NIR.P90	NIR.P90
Elev.P95	NIR.P95	NIR.P95
Elev.P99	NIR.P99	NIR.P99
Canopy.relief.ratio	Red.minimum	Red.minimum
Percentage.all.returns.above.2.00	Red.maximum	Red.maximum
All.returns.above.2.00	Red.stddev	Red.stddev
All.returns.above.mean	Red.variance	Red.variance
	Red.CV	Red.CV
	Red.skewness	Red.skewness
	Red.kurtosis	Red.kurtosis
	Red.P01	Red.P01
	Red.P05	Red.P05
	Red.P20	Red.P20

Difference spatial metrics computed from pre and post fire aerial images	Difference spectral and spatial metrics computed from pre and post fire aerial images	Difference spectral metrics computed from pre and post fire aerial images
	Red.P25	Red.P25
	Red.P30	Red.P30
	Red.P40	Red.P40
	Red.P50	Red.P50
	Red.P60	Red.P60
	Red.P80	Red.P80
	Red.P90	Red.P90
	Red.P95	Red.P95
	Red.P99	Red.P99
	Green.minimum	Green.minimum
	Green.maximum	Green.maximum
	Green.mean	Green.mean
	Green.stddev	Green.stddev
	Green.variance	Green.variance
	Green.CV	Green.CV
	Green.skewness	Green.skewness
	Green.kurtosis	Green.kurtosis
	Green.P01	Green.P01
	Green.P05	Green.P05
	Green.P10	Green.P10
	Green.P20	Green.P20
	Green.P25	Green.P25
	Green.P30	Green.P30
	Green.P40	Green.P40
	Green.P50	Green.P50
	Green.P60	Green.P60
	Green.P70	Green.P70
	Green.P75	Green.P75
	Green.P80	Green.P80
	Green.P90	Green.P90
	Green.P95	Green.P95
	Green.P99	Green.P99
	Green.P95	
	Elev.stddev	
	Elev.variance	
	Elev.CV	

	Difference spectral and spatial metrics computed from pre and post fire aerial images
	Elev.skewness
	Elev.kurtosis
	Elev.P01
	Elev.P05
	Elev.P10
	Elev.P20
	Elev.P25
	Elev.P30
	Elev.P40
	Elev.P50
	Elev.P60
	Elev.P70
	Elev.P75
	Elev.P80
	Elev.P90
	Elev.P95
	Elev.P99
	Canopy.relief.ratio
	Percentage.all.returns.above.2.00
	All.returns.above.2.00
	All.returns.above.mean
	Total.return.count